Additives in Metal Halide Perovskite Films and Their Applications in Solar Cells

Zonghao Liu[a,+], Luis K. Ono[a,+], Yabing Qi[a,*]

[a] *Energy Materials and Surface Sciences Unit (EMSSU), Okinawa Institute of Science and Technology Graduate University (OIST), 1919-1 Tancha, Onna-son, Kunigami-gun, Okinawa, 904-0495, Japan*

[*]Corresponding author: Yabing Qi, *E-mail address:* Yabing.Qi@OIST.jp

+These authors contributed equally to this work

Abstract:

The booming growth of organic-inorganic hybrid lead halide perovskite solar cells have made this promising photovoltaic technology to leap towards commercialization. One of the most important issues for the evolution from research to practical application of this technology is to achieve high-throughput manufacturing of large-scale perovskite solar modules. In particular, realization of scalable fabrication of large-area perovskite films is one of the essential steps. During the past ten years, a great number of approaches have been developed to deposit high quality perovskite films, to which additives are introduced during the fabrication process of perovskite layers in terms of the perovskite grain growth control, defect reduction, stability enhancement, etc. Herein, we first review the recent progress on additives during the fabrication of large area perovskite films for large scale perovskite solar cells and modules. We then focus on a comprehensive and in-depth understanding of the roles of additives for perovskite grain growth control, defects reduction, stability enhancement. Further advancement of the scalable fabrication of high-quality perovskite films and solar cells using additives to further develop large area, stable perovskite solar cells are discussed.

Keywords: Perovskite solar cell; Additive; Solar modules; Film quality

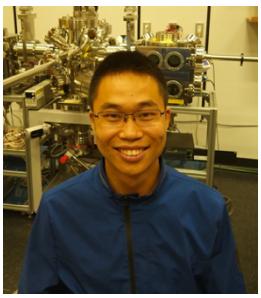

Zonghao Liu received his B.Sc. in 2011 and Ph.D. in 2016 from Huazhong University of Science and Technology, China. He was a visiting student in University of California, Los

Angeles, USA, in 2015. From 2016 to 2017, he was a research assistant in Peking University, China. He is currently a postdoctoral scholar in Prof. Yabing Qi's Research Unit at Okinawa Institute of Science and Technology Graduate University in Japan. His current research focuses on electronic devices based on inorganic/organic perovskites, especially on perovskite solar cells.

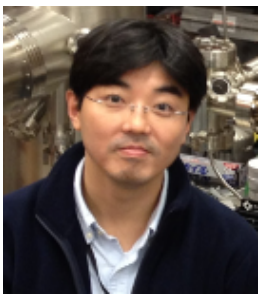

Luis K. Ono is a staff scientist in Prof. Yabing Qi's Research Unit (Energy Materials and Surface Sciences Unit) at Okinawa Institute of Science and Technology Graduate University in Japan. He obtained his B.S. in Physics/Microelectronics from the University of São Paulo, Brazil. Later he joined the Department of Nuclear Engineering in Kyoto University, Japan, and the University of Central Florida, USA, where he obtained his M.S. and Ph.D., respectively. His current research focuses on the fundamental understanding and surface science aspects of perovskite solar cells.

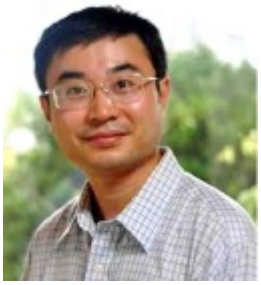

Yabing Qi is Professor and Unit Director of Energy Materials and Surface Sciences Unit at Okinawa Institute of Science and Technology Graduate University in Japan. Prior to his current appointment, Prof. Qi was a postdoctoral fellow at Princeton University. He received his B.S., M.Phil., and Ph.D. from Nanjing University, Hong Kong University of Science and Technology, and University of California Berkeley, respectively. Prof. Qi is a Fellow of the Royal Society of Chemistry, and is currently on the editorial board of *JPhys Materials* (IOP Publishing). His research interests include perovskite solar cells, surface sciences, energy materials, and organic electronics (https://groups.oist.jp/emssu).

1. Introduction

Organic-inorganic hybrid lead halide perovskite solar cells (PSCs) have been recognized as promising photovoltaic technology that is approaching commercialization [1-6]. Although small-size PSCs have achieved certified power conversion efficiency (PCE) comparable with crystalline silicon solar cells [7], they are still facing issues before coming into practical application, such as scalable fabrication, long-term stability etc.[6, 8, 9] One of the most important targets for the development of PSCs is to achieve high-throughput manufacturing of high efficiency stable large-area perovskite solar modules. In general, a PSC consists of a conductive transparent substrate, electron/hole transport layers, back contact electrode and perovskite layer. The fabrication of transparent conductive substrates, electron/hole transport layers, and back contact electrodes can be readily achieved thanks to the massive accumulated experience in semiconductor industry and electronic devices. For organic-inorganic hybrid lead halide perovskites (denoted as perovskites throughout this review), their unique synthetic chemistry makes the film quality of the perovskite layer to be dictated to a large degree by the deposition process, which heavily influences the device performance of PSCs [10]. The fabrication of large-area, high quality, and uniform perovskite films are recognized as one of the most essential technical bottlenecks for fabricating high efficiency and stable perovskite solar modules. During the past decade, a great number of film formation approaches have been developed to fabricate perovskite films with large area [10-13]. Among these film formation approaches, the introduction of additives into the precursors, i.e., additive engineering, during the film formation process has been demonstrated to be an effective strategy to fabricate high quality perovskite films. Additive engineering effectively affects the film quality of perovskite layers in terms of the perovskite grain growth control, defect reduction, stability enhancement, etc.

In this review article, we focus on bulk film additives in perovskite films and their applications in solar cells. The bulk film additives are defined as the compounds added into the perovskite precursor solution acting as exotic species that do not participate in the formation of the perovskite crystal structure but keep a certain concentration in the final perovskite bulk films as foreign species. In Section 2, we discuss the recent progress on the use of additives in the fabrication of large area perovskite films for large scale perovskite solar cells or modules. In Section 3, a comprehensive and in-depth understanding of the roles of additives on perovskite morphology control is reviewed. In Section 4, the additives used for defect density reduction/passivation in perovskite films are discussed. In Section 5, the use of additives for perovskite films stability enhancement is reviewed. In the last section, Section 6, a conclusion and outlook about the use of bulk film additives to further facilitate the development of the

scalable fabrication of high-quality perovskite films and large area, stable solar cells will be given.

2. Additives for large area perovskite solar cells and modules

Although small-size PSCs have achieved high efficiencies over 25%, the efficiency of large-area PSCs is still lagging behind small-size devices [7]. The film quality of perovskite films on large-scale substrate was recognized to be one of the most important bottlenecks for efficiency improvement of large-area PSCs. To date, a number of film formation strategies via the spin coating method have been developed to deposit uniform perovskite films for small-size high efficiency PSCs. However, it was challenging to deposit uniform perovskite films across large areas for high efficiency large area PSCs and modules by the commonly used spin coating method due to the intrinsic film formation mechanism. Besides, the spin coating method showed a high precursor solution waste ratio over 90% [14], which may negate the low-cost advantage of PSCs. Therefore, the realization of scalable fabrication of high-quality and uniform large-area perovskite films with scalable processing techniques is one of the essential steps. Several recent review papers have reviewed recent progress on scalable fabrication of PSCs [5, 15-17]. A further improvement of film quality of large-area perovskite films via scalable processes, such as spray-coating, doctor-blade coating, slot-die coating is required to accelerate the development of scalable PSCs. Considering the accumulated massive successful experience in fabrication of high-quality perovskite films via additive engineering for small-size PSCs, additive engineering is believed to be an effective strategy to obtain high-quality large area perovskite films for efficient large area PSCs and modules, in terms of the perovskite grain growth, defect reduction, stability enhancement. In this section, we will review recent progress on the fabrication of large area perovskite solar cells and modules via additive engineering.

To fabricate high efficiency large PSCs and solar modules, the first requirement is to deposit smooth and uniform perovskite films with full coverage on substrates. Huang and co-workers added a small amount (tens of parts per million) of surfactants (for example, L-α-Phosphatidylcholine) into the $MAPbI_3$/DMF ($MAPbI_3$ is $CH_3NH_3PbI_3$ and DMF is N,N-dimethylformamide) precursor solution and deposited perovskite films via the doctor blading method [18]. The authors found that surfactant additive not only altered the fluid drying dynamics to suppress solution flow, but also improved the wettability of the perovskite ink on the underlying non-wetting charge transport layer [18]. With surfactant additive engineering, the authors demonstrated a fast deposition of smooth perovskite films with a root-mean-square

roughness of 14.5 nm via blade coating at a coating rate of 180 m h^{-1}. Their doctor blade coated perovskite solar module showed stabilized aperture module efficiencies of 15.3% (33.0 cm^2) and 14.6% (57.2 cm^2), respectively.

The fabrication of perovskite films with high crystallinity, low defect density, high mobility, long charge diffusion length, low charge recombination is equally essential as film uniformity to further improve the efficiency of large area PSCs and solar modules. The accumulated experience of optimizing these intrinsic features of perovskite films using additives in small size PSCs is likely to be helpful for large area PSCs and solar modules [19, 20]. Chlorine related additives have been widely used as an efficient strategy to fabricate high quality perovskite films since the early stage of PSCs [21]. This strategy has also been successfully transferred into scalable manufacturing of large area PSCs and modules. For example, Chang, Kanatzidis, Marks and co-workers deposited high-quality perovskite films via the hot-casting process by adding a small amount of $PbCl_2$ + MACl as additive into the PbI_2 + MAI precursor solution with controlled Cl^- incorporation. Similar to its function in small size PSCs, Cl^- incorporation increases carrier diffusion length, improved perovskite film morphology and reduced recombination [22]. The 5 cm × 5 cm eight-cell module delivered an active-area PCE of 12.0% [22]. Together with solvent engineering, Zhu and co-workers added MACl into the $MAPbI_3$/(NMP : DMF = 9:8 (v:v)), where NMP is N-Methyl-2-pyrrolidone, precursor solution to deposit perovskite films on TiO_2/fluorine-doped tin oxide (FTO) substrates via the doctor blading method [23]. They demonstrated that the additive MACl could largely facilitate recrystallization and shorten the annealing time to obtain high-quality perovskite films. The solar module has a total area of 12.6 cm^2 and an active area of 11.09 cm^2 with an active-area PCE of 14.06% from the reverse scan, with a stabilized active-area PCE of 13.3%. Recently, Qi and co-workers introduced MACl into a gas-solid reaction based perovskite formation method to fabricate over 1 μm thick high-quality perovskite films [24]. Cl^- incorporation was shown to increase charge diffusion length, mobility and reduce recombination, which ensured efficient charge collection across such thick perovskite films. The 5 cm × 5 cm solar module with an active area of 12 cm^2 yielded an active area PCE of 15.3% with high device reproducibility and the corresponding small size PSC showed good stability (T80 ~ 1600 h).

Some research groups reported that H_2O was harmful for perovskite solar cells, due to the easy decomposition of perovskite films under a humid environment [25]. On the other hand, some other groups also found that a suitable amount of water could facilitate nucleation and

crystallization of the perovskite material, resulting in improved perovskite film quality and enhanced device performance [26]. Chang and co-workers reported a high quality perovskite formation strategy by the synergistic effect of the H_2O additive and DMF vapor treatment via a two-step spin coating method [27]. They found that a small amount of H_2O additive helped MAI penetrate into the thick PbI_2 films to form a thick film with a pure $MAPbI_3$ phase and produced larger grains by slowing down the perovskite crystallization rate, and also enlarged grain size with cooperation of DMF vapor. Their large-area high-quality, 500 nm thick perovskite films delivered an efficiency of 16.7% and 15.4% for the 1.3 cm^2 PSCs and 11.25 cm^2 mini-module, respectively.

Inspired by the results of 1,8-diiodooctane (DIO) as the additives in small size PSCs [28], Fu and co-workers reported using DIO as additive to control the perovskite crystal growth for perovskite solar modules [29]. Their 5 cm × 5 cm solar module gave a PCE of 11.2% on the active area of 12 cm^2.

Furthermore, alkali metal salts have been demonstrated to be useful additives to control perovskite film formation, passivate defects and enhance stability for high efficiency PSCs. Bu and co-workers incorporated potassium (K) into CsFAMA (FA is formamidinium) mixed cation based perovskites films to promote perovskite crystallization [30]. Similar to the related reports in small size PSCs [31-33], K incorporation led to a lower interface defect density, longer carrier lifetime and faster charge transport. Their 6 cm × 6 cm solar module achieved a high active area efficiency of 15.76% without hysteresis. Besides solution processing, the hybrid chemical vapor deposition (HCVD) process for perovskite fabrication is also scalable and can be used to fabricate large area perovskite solar modules [34, 35]. Inspired by using Cs additives in solution processing method-based FA cation perovskite fabrication, Cs additive engineering has also been applied to fabricate large area FACs mixed cation perovskite films via HCVD, which has been shown to be effective leading to enhanced thermal and phase stability [36, 37]. Cs remains in the final perovskite film, which is different from the case of K (See Section 3).

The additive of 5-ammoniumvaleric acid (5-AVA) iodide has been reported to largely enhance the perovskite film quality in the mesoporous oxide frame of fully printable carbon electrode-based hole transport materials (HTM) free PSCs. Due to the advantage of the screen-printing process, upscaling of this kind of device using 5-AVA additive based $MAPbI_3$ has been successfully achieved showing good performance and outstanding long-term stability [38-40]. In this section, we review the recent progress on the fabrication of large area PSCs and modules via additive engineering. In the subsequent section, we discuss about the perovskite

morphology control by the use of additives, which has implications on the perovskite film quality.

Table 1. Selected works reporting perovskite film growth aiming at solar cell devices with active areas larger than 10 cm^2. The PCE values are normalized by the active area (denoted as ^{ac}), aperture area (denoted as ^{ap}), designated area (active area + dead area for interconnections) (denoted as ^{da}). Certified efficiency is denoted as ^{CE}. Stabilized PCE is denoted as ^{S}. Substrate area is denoted as ^{sa}.

Additive	Perovskites	Perovskite film fabrication method	PCE	Cell or module size (cm^2)	Additive detected?	Main conclusion	Years Ref.
L-α-Phosphatidylcholine	$MAPbI_3$	doctor blading	15.3%$^{ap+S}$	6 × 15^{sa} (33.0^{ap})		additive suppress solution flow and improve wettability	2018 [18]
			14.6%$^{ap+S}$	6 × 15^{sa} (57.2 ^{ap})		Additive reduce annealing time	
MACl	$MAPbI_{3-x}Cl_x$	Spin coating /hot casting	12%^{ac}	5 × 5 ^{sa} (GFF ~0.6)	Cl detected by SEM-EDS	Cl enhanced film quality	2016 [22]
MACl	$MAPbI_3$	Doctor blading	14.06^{ac} (13.3%$^{ac+s}$)	12.6^{da} (11.09^{ac})	N/A	Cl facilitate grain growth	2018 [23]
MACl	$MAPbI_3$	Spin coating/gas-solid reaction	15.3%^{ac}	5 × 5 ^{sa} (12^{ac})	Cl detected by SIMS	Cl enhanced film quality	2018 [24]
H_2O	$MAPbI_3$	Spin coating	15.4%^{ac}	5 × 5 ^{sa} (11.25^{ac})		H_2O additive enhanced	2017 [27]

						film quality	
DIO	$MAPbI_{3-x}Cl_x$	Spin coating	11.2%[ac]	5 × 5 [sa] (12[ac])		DIO control perovskite growth	2017 [29]
KI	$K_xCs_{0.05}(FA_{0.85}MA_{0.15})_{0.92}Pb(I_{0.85}Br_{0.15})_3$	Spin coating	15.76%[ac]	6 × 6[sa] (20[ac])			2017 [30]
CsBr	$Cs_{0.1}FA_{0.9}PbI_{2.9}Br_{0.1}$	HCVD	10.37%[ac] (9.34%[da])	10 × 10[sa] (46.7[ac])		CsBr enhanced thermal, phase stabilities	2019 [36]
CsBr	$Cs_{0.24}FA_{0.76}PbI_{3-y}Br_y$	HCVD	12.24%[ac]	8 × 8[sa] (41.25[ac])		CsBr moisture, thermal stability	2018 [37]
5-AVA	MA(5-AVA)PbI_3	Screen printing	10.5% [ac]	5 × 10[sa] (31[ac])			2016 [38]
5-AVA	MA(5-AVA)PbI_3	Screen printing	10.7% [ac]	10 × 10[sa] (70[ac])			2016 [38]
5-AVA	MA(5-AVA)PbI_3	Screen printing	10.4% [ac]	10 × 10[sa] (49[ac])			2017 [39]
5-AVA	MA(5-AVA)PbI_3	Screen printing	11.2% [ac]	10 × 10[sa] (46.7[ac])			2017 [40]

3. Additives that improve perovskite film morphology

The optimization of perovskite film morphology, such as film coverage, roughness, grain size and grain boundaries, has been recognized to be extremely important to achieve high efficiency since the early stage of PSCs [12, 41, 42]. This is because uniform morphology avoids shunt paths, enlarges light harvesting, and helps improve the quality of adjacent charge transport layers. As discussed in Section 2, the accumulated understanding of perovskite film formation obtained through the studies on small area PSCs can help further optimize the perovskite film formation on large scale [10, 11, 13, 16, 42]. It is necessary to have an in-depth understanding of the film formation mechanism to guide the application of these accumulated understanding. In the following, we first review the mechanism of perovskite film growth in

Section 3.1 and then review the progress on additive engineering towards improved perovskite film morphology in Section 3.2.

3.1 Mechanism of perovskite film formation

As discussed above, film quality largely affects device performance. A delicate control of film morphology is thus critical for device performance. In this section, we give a general introduction to the mechanism of perovskite film formation to provide a fundamental understanding of the film formation process, which guides the use of additives that help control the perovskite films quality. In general, the perovskite film formation based on the one-step method contains the following steps: i) deposit the precursor solution onto a substrate, ii) dry the wet film to reach supersaturation followed by nucleation and growth, and iii) thermal annealing to facilitate further film growth. The second step is usually recognized to be the most vital to control the obtained film quality, several review papers have provided detailed discussions on the related mechanisms [10, 11, 16, 42]. This step is generally applicable to a nucleation/growth crystallization mechanism. A La Mer model can be applied to illustrate the involved three stages as shown in Fig. 1a. In the first stage, the concentration of the precursor solution is below the minimum concentration for nucleation (C_{Smin}), the solute is well dissolved in the solution, and no appreciable nucleation occurs. In the second stage, the concentration gradually increases and reaches the supersaturation limit (the minimum concentration for nucleation) as the solvent is continuously removed from the deposited solution. The removal of solvent in the perovskite precursor solution can be driven by thermal annealing, gas blowing, pumping or antisolvent extraction. At this stage, the nucleation occurs, forming nuclei along with their growth. As nucleation progresses, the solute is gradually consumed. When the solution concentration gradually decreases to be lower than C_{Smin}, film formation comes into the third stage, in which the nucleation terminates, but the crystallites continue to grow. As the concentration further reduces close to the solubility Cs, the crystal growth is suppressed

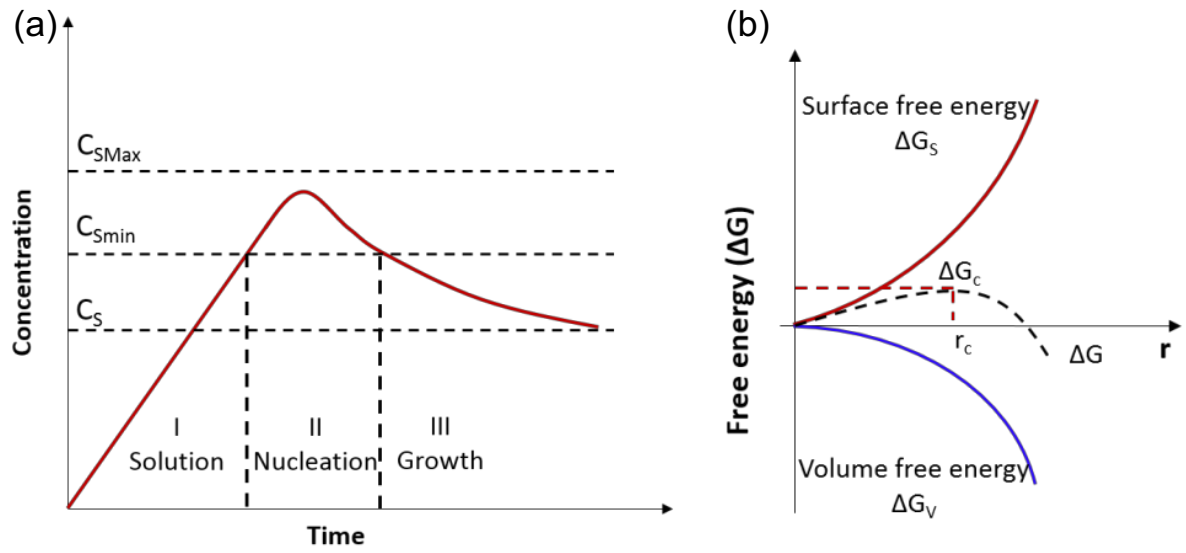

Fig. 1. (a) La Mer diagram for homogeneous nucleation. Cs is the solubility, C_{Smin} is the supersaturation limit (the minimum concentration for nucleation), C_{Smax} is the critical limiting supersaturation (the maximum concentration for nucleation). The regions I, II, and III represent solution, nucleation and growth, respectively. (b) Schematic diagram of the classical free energy (ΔG) diagram for homogeneous nucleation as a function of particle radius (r). ΔG_s is the surface free energy, ΔG_v is the bulk free energy. ΔG_c is critical free energy, and r_c is critical radius of nucleus [10].

In the classical nucleation model, the nucleation events without nucleation sites, i.e., homogeneous nucleation can be described by $\Delta G = \frac{4}{3}\pi r^3 \Delta g + 4\pi r^2 \delta$, where r is sphere radius, the first term is bulk free energy (ΔG_V) during nucleation, which is always negative when nucleation occurs, see the blue curve in Fig. 1b; the second term is interface energy (ΔG_S) at the surface of the nucleus, where δ is the surface tension, ΔG_S is always positive, see the red curve in Fig. 1b. From the above equation, when nuclei radii r is larger than the critical radius of nucleus r_c, the nuclei is thermodynamically stable and tends to grow; when r is smaller than r_c, nuclei dissolves back into solution. When depositing a perovskite film on a substrate, heterogeneous nucleation should also be considered due to the existence of foreign surface acting as nucleation sites. The energy barrier of heterogeneous nucleation (ΔG_{hetero}) can be corrected as: $\Delta G_{hetero} = f(\theta)\Delta G_{homo}$, $f(\theta) = \frac{(2+cos\theta)(2+cos\theta)^2}{4}$, where θ is the contact angle of the precursor solution on the substrate. A low density of nuclei tends to form discontinuous morphologies such as island-like crystals, which is detrimental to device performance. Thus, a high density of heterogeneous nuclei on the substrate is essential to form a uniform and full

coverage film on the substrate. According to the above equations, the nucleation can be tuned by controlling the experimental parameters such as temperature, supersaturation level, surface energy and wettability of the substrate. Although the above classical nucleation/growth theory provides a simple system to understand perovskite formation, the real perovskite formation actually involves more complicated factors, because of multiple physico-chemical parameters and dynamics (e.g., presence of multiple ions, complexity of polar aprotic solvents, overlap between nucleation and growth processes, etc.) and evolving intermediates [10]. The description above just provides a general understanding of perovskite formation. Detailed discussions about perovskite formation can be found in several review papers focusing on this topic [10, 11, 16, 42]. In the next section (Section 3.2), we review recent progress on the fine controlling of the perovskite film morphology by using additives.

3.2 Perovskite film growth engineering using additives

As described above, perovskite growth can be tuned by controlling the parameters that govern the perovskite formation kinetics. Additives added into the precursor solution can interact with the solute, solvent or the substrate to tune the perovskite formation by affecting the experimental parameters such as temperature, supersaturation level, surface energy and wettability of the substrate. Additives engineering is thus an effective strategy to control the film quality of the obtained perovskite layer. In this section, we review recent progress on the additive engineering to improve perovskite film morphology such as surface uniformity, coverage, and grain size by using different additives including: 1) organic halide ammonium salt additives; 2) polymer additives; 3) metal salt additives; 4) other monovalent noble metal cation salts; 5) bivalent metal cation salts; 6) trivalent cation salts.

3.2.1. Organic halide ammonium salt additives.

Organic ammonium salts, such as MA halide, FA halide are the most widely used components of perovskite structure. Organic ammonium salts as well as their analogues can also be used as additives into the perovskite precursor solution to modulate the perovskite formation process making use of their strong interaction with the perovskite species or their temporarily incorporation into the intermediate template. Besides, some organic ammoniums containing larger organic groups can form low-dimensional or mixed dimensional perovskites. Apart from the morphology optimization, these additives are more likely to show positive effects on the stability enhancement of perovskites, which is discussed in Section 5.

Among these organic ammonium salt additives, MACl can be considered as one of the most widely used additives for high quality perovskite film formation [43]. Zhao and co-workers reported the use of MACl additive into the $MAPbI_3$ precursor solution with different molar ratios and showed improvement in device performance (Fig. 2a) [44]. They found that the color of $MAPbI_3$ films changed slowly with the increasing MACl content, implying the formation of a temporary intermediate phase $MAI{\cdot}PbI_2{\cdot}MACl$ retarding the crystallization process (Fig. 2b). This is consistent with the observations by Pang and co-workers about the crystallization process of the films with and without the MACl additive via *in situ* microscopy as shown in Fig. 2c [45]. After the subsequent thermal annealing, most MACl was removed due to its low sublimation temperature [24, 46]. Pure perovskite films with enhanced absorption and improved coverage were obtained, leading to improved device performance. Besides retarding of nucleation by using the MACl additives, MACl was also found to interact with the colloidal clusters to enlarge their size in the perovskite precursor solution [47]. By taking advantage of the synergetic effect of dimethyl sulfoxide (DMSO) that stabilizes formation of enlarged clusters, orderly arranged large size colloidal clusters can form monolayer wet intermediate phase films on the substrate, which after annealing can be transformed into high crystalline perovskite films with enlarged large grains with an average grain size of 3 μm. Regarding the Cl incorporation into perovskite films, the debate on the existence of chlorine in the resultant films is still not completely settled. To date, an extensive number of analytical tools, such as X-ray photoelectron spectroscopy (XPS) [48-50], angle-resolved XPS (AR-XPS) [51], XPS depth-profile [52], hard XPS (HAXPS) [53], fluorescence yield X-ray absorption spectroscopy (FY-XAS) [53], time-of-flight secondary ion mass spectrometry (TOF-SIMS) [48], *in situ* XRD [54, 55], glazing-incidence XRD (GIXRD), X-ray absorption near edge structure (XANES) [54, 56], energy-dispersive X-ray spectroscopy (EDX or EDS) [50, 54, 55], X-ray fluorescence spectroscopy (XRF) [54], grazing-incidence wide-angle X-ray scattering (GIWAXS) [54], photothermal-induced resonance (PTIR) [57], Kelvin probe force microscopy (KPFM) [58], thermogravimetric analysis (TGA) [50], ion chromatography [59] and other techniques have been used to detect the presence of Cl in perovskite [21]. The recent work by Qi and co-workers also confirmed the chlorine incorporation by SIMS in MACl-additive-based perovskite films with a thickness over 1 μm [24]. Due to the large ionic radii difference between Cl^- and I^-, it is thermodynamically unfavorable to form perovskites with a high ratio of Cl. There is namely no obvious ion substitution of I^- with Cl^- [24]. In some cases, the content was even lower than the signal detection limits of some analytical tools. The resulted perovskite films thus did not exhibit an obvious blue-shifted bandgap. The excess MACl partially

compensated the MA^+ vacancy defects, and a low density of Cl incorporation improved the optoelectronic properties of perovskites. Besides $MAPbI_3$, MACl has also been reported as an additive to improve the morphology and also phase stability of FA [60, 61] and FA/MA based perovskites [4, 62, 63], and achieved high PCEs. Other kinds of organic halide ammonium salts, such as ammonium chloride [64-66], guanidinium iodide [67], methylammonium thiocyanate [68], ammonium thiocyanate [69, 70], methylammonium acetate [71], ammonium acetate [72] have also been used as additives to control the perovskite film morphology. Other larger-size ammonium salts that induced the formation of 2D or 2D/3D structure perovskite are not discussed here, because these salts did not function as additive but were directly incorporated into the perovskite structures.

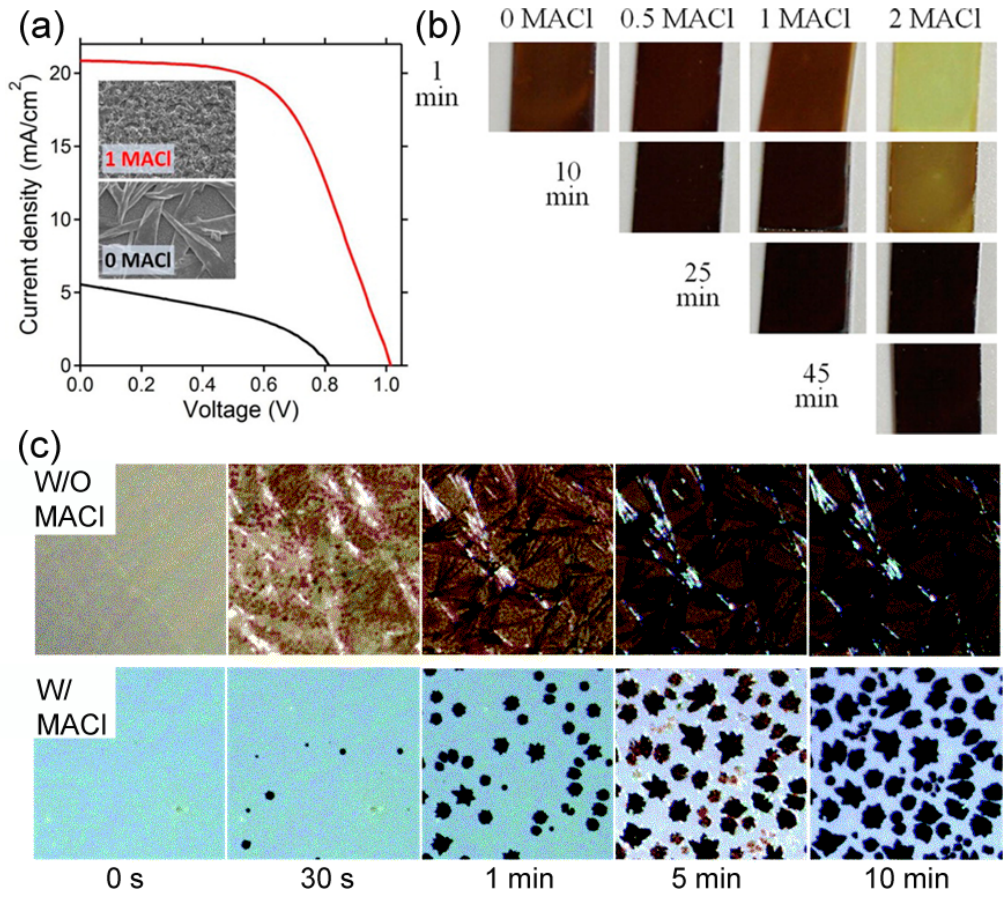

Fig. 2. (a) J-V curves and morphology and (b) optical images of the perovskite films prepared from $CH_3NH_3PbI_3$ precursors with different amounts of MACl and annealed at 100 °C with varying duration (as indicated). Reproduced with permission from ref. [44]. Copyright 2014, American Chemical Society. (c) In situ microscopy images of the crystallization process of the films fabricated from $MAPbI_3$ precursor solutions with and without the MACl additive. Reproduced with permission from ref. [45]. Copyright 2017, The Royal Society of Chemistry.

3.2.2. Polymer additives.

Different from organic ammonium salts that substitute the organic ammonium and halide to interact with perovskites via strong chemical interactions, polymer additives that are functionalized with some atoms or functional groups could form hydrogen bonds with perovskites or contain electron donating groups that can interact with lead ions. This kind of interaction affects the perovskite growth/nucleation process and leads to fine-tuned morphology. Su and co-workers added 1 wt % of poly(ethylene glycol) (PEG) in the $MAPbI_3$ perovskite precursor solution to tune the morphology of the perovskite layer, leading to PCE improvement from 10.58% to 13.2% [73]. This improvement was because PEG not only help the perovskite precursor spread out smoothly, but also retarded the growth and aggregation of perovskite crystals and reduced the voids between perovskite domains. The interaction of PEG with perovskite was further evidenced in the work by Zhao and co-workers, where the O atoms in PEG can interact with MA^+ via hydrogen bonds [74]. Grätzel and co-workers used poly(methyl methacrylate) (PMMA) as a template to control nucleation and crystal growth of $(FAI)_{0.81}(PbI_2)_{0.85}(MAPbBr_3)_{0.15}$ perovskite, where the carbonyl groups in PMMA formed an intermediate adduct with PbI_2 revealed by Fourier transform infrared spectroscopy (FTIR) [75]. PMMA also facilitated heterogeneous nucleation over the perovskite precursor film, leading to improved grain size and perovskite growth along certain preferred directions. As a result, they obtained shiny smooth perovskite films of excellent electronic quality, a high efficiency of 21.6% and a certified PCE of 21.02%. Other polymers such as amine-polymer poly[(9,9-bis(3′-(N,N-dimethylamino)propyl)-2,7-fluorene)-alt-2,7-(9,9-dioctylfluorene)] [76], polyvinylpyrrolidone [77], polymer polyacrylonitrile [78] have also been reported to act as additives to tune the perovskite morphology. Another important advantage of polymer additives is that they can enhance the stability of the perovskite layer by strong interaction with perovskites and also their hydrophobicity. This topic is discussed in Section 5. In terms of morphology control, the current polymer additives are based on common polymers. To further enlarge the advantages of polymer additives, it is desirable to explore novel polymer additives with unique molecular structures or specific functional groups to precisely control the interaction between polymer and Pb^{2+} ions (or organic ammonium) during the film formation process.

3.2.3. Metal salts additives.

Metal salts are another kind of important additives to tune the morphology of perovskite films. A small amount of Cs^+ can partially substitute FA^+ or MA^+ to form high quality 3D

perovskite films and achieve high efficiency. Its alkali analogues such as Rb^+, K^+ Na^+ based salts have also been introduced into perovskite films, but these alkali ions are different from Cs^+. These alkali ions were only present in the perovskite films in the form of additives due to their much smaller sizes, which did not fulfill the ion size requirement to form a 3D perovskite structure. Chu and co-workers reported using KCl, NaCl and LiCl as additives to form perovskite film via a two-step method, and the first two led to much improved PCEs [79]. They proposed that these alkali metal halides chelated with Pb^{2+} ions and enhanced the crystal growth of PbI_2 films, resulting in nanostructured morphologies. The nanostructured PbI_2 films thus affected nucleation and growth of perovskite films. Interestingly, XPS measurement results suggested that the resultant film showed a clear alkali ion signal but a negligible chlorine signal, which may be due to the similar reasons mentioned above for the MACl case (i.e., the evaporation of Cl from the perovskite films during annealing or the chlorine content is below the XPS instrument detection limit). Durstock and co-workers added NaI into the $MAPbI_3$ perovskite precursor and with a synergistic effect of solvent annealing, the resultant perovskite films showed enlarged grain size than the films without additives [80]. They proposed that Na^+ ions promoted nucleation resulting in small perovskite grains. The mobile small Na^+ ions were also likely to facilitate grain boundary mobility, enabling the growth of larger grains during the solvent annealing process. They also compared NaI with NaBr. The latter also showed a similar effect on grain size enhancement. Recently, NaF has been introduced as additive into $(Cs_{0.05}FA_{0.54}MA_{0.41})Pb(I_{0.98}Br_{0.02})_3$ perovskite. The authors also compared NaF with NaCl and NaBr. Only slightly enlarged grain size was observed, but the hydrogen bond interaction between F and organic ammonium was proposed to enhance both film quality and stability [81]. Rb salts have also been used as additives into CsFAMA perovskite precursors, and the resultant perovskite films showed enlarged grain size with suppressed non-radiation recombination leading to enhanced Voc and PCE [82]. K^+ based salts have also been added into the perovskite precursor solution to tune the perovskite growth and also electronic properties of perovskite, which led to improved efficiency and suppressed hysteresis [31-33]. In addition, there were reports about adding multiple alkali based salts to tune the perovskite film quality [30, 83]. Although these alkali salts have been successfully used as additives to tune the morphology leading to improved efficiency, where these alkali ions reside in the bulk of perovskite films is still an unresolved question. For example, Stranks and co-workers have proposed that K^+ ions are not incorporated into the perovskite lattice, but are mainly located at the grain boundaries [33]. The excess iodide ions compensated halide vacancies and passivated the non-radiative recombination pathways. A more systematic study was done by Emsley and co-workers [84].

They used solid-state magic-angle spinning (MAS) nuclear magnetic resonance (NMR) spectroscopy to probe microscopic composition of Cs-, Rb-, K-, MA-, and FA-containing phases in double-, triple-, and quadruple-cation lead halides in bulk and in a thin film. They also found no proof of Rb or K incorporation into the 3D perovskite lattice in these systems except Cs.

Other monovalent noble metal cation salts have also been used as additives to prepare perovskite films. Friend and co-workers reported that the addition of monovalent noble metal cation salts (e.g., CuBr, CuI, and AgI as well as NaI) into the PbI_2 precursor solution in a two-step perovskite formation process [85]. They found that the introduction of these additives largely affected the morphology of PbI_2 films and perovskite films, where a continuous coverage and uniform film for the films containing CuI and AgI additives and a better conversion from PbI_2 to $MAPbI_3$ perovskite for the films containing NaI and CuBr additives. They also observed by XRD that these metal cation ions were not incorporated into the perovskite lattice. Device performance improvement was attributed to the trap state passivation by these additives.

Besides monovalent metal cation salts, bivalent metal cation salts with the same ionic charge number of B sites (such as Pb^{2+}, Sn^{2+}) of ABX_3 perovskites, have also been added into the perovskite precursor as additives. Jen and co-workers added four transition metals, Mn, Fe, Co, and Ni, in the form of divalent halides into the $MAPbI_3$ precursor solution [86]. Comparing to a rod-like morphology of the pure $MAPbI_3$ without additives in DMSO, the addition of transition metals resulted in more isotropic leaf-like morphology. The interference of the CH_3NH_3I-PbI_2-DMSO complex in the presence of the transition metals leads to direct perovskite nucleation, which is responsible for the leaf-like morphology. XRD results suggested that these transition metals might be incorporated into the films. However, the small shifts of the lattice parameter by adding these transition metals suggested that it was unlikely for these transition metals to directly substitute Pb. An additional effect of the presence of the transition metals, under the impact of magnetic fields (e.g., the effect of the magnetic stir-bar in hot plate) were also explored. A stronger magnetic field induced larger grains and better coverage, and also twinning features. Among these four transition metals, Mn was the only one that did not induce deep trap states and was a promising additive beneficial for the optoelectronic properties of perovskite films. Qi and co-workers introduced Mn^{2+} as additive into a $CsPbIBr_2$ film and found that Mn-doped all-inorganic perovskite film showed better crystallinity and morphology than its undoped counterpart, and led to better photovoltaic performance [87]. Moon and co-workers also found that the $CuBr_2$ additive increased the

average grain area/maximum grain area of resultant $MAI(PbI_2)_{1-x}(CuBr_2)_x$ films and led to improved device performance [88]. This improvement was attributed to the formation of the $CuBr_2 \cdot DMSO_2$ complex, which changed into the liquid phase during annealing due to the separated melting and decomposition of the complex, promoting the crystal growth of $MAI(PbI_2)_{1-x}(CuBr_2)_x$ perovskite during annealing. Their DFT results illustrated the possibility of Cu-doping and its positive effect on conductivity due to effective dopants enhancing charge carrier density supported by capacitance-voltage characteristics.

Liao and co-workers introduced trivalent cation In^{3+} in the form of chloride salts into $MAPbI_3$ perovskite, which led to improved device performance.[89] They found that the $InCl_3$ additive largely affected the grain growth and formed perovskite films with high coverage, fewer pinholes, but much smaller grain size. This additive was also verified to make the perovskites grow along multiple directions by grazing incidence X-ray diffraction (GIXRD). The high-resolution GIXRD based on high brightness synchrotron radiation X-ray source was used to clarify the partial Pb^{2+} substitution by In^{3+}. Although the $MAPbI_xCl_{3-x}$ did not show the existence of chlorine based on XPS measurements, the $InCl_3$-additive-incorporated perovskite films showed clear Cl XPS and In peaks, verifying the presence of In and Cl in the final $MAPb_{0.85}In_{0.15}I_3Cl_{0.15}$ perovskite films. The presence of Cl also benefited the minimization the morphological and energetic disorder of the perovskite films, led to improved device performance. Other trivalent cations, such as Al^{3+}, have also been used as additives in perovskite films to improve device performance by Snaith and co-workers.[90] Although the XRD results suggested that Al^{3+} is not incorporated into the perovskite lattice due to the much smaller ionic radius than Pb^{2+}, but the presence of a small amount of Al^{3+} in the perovskite growth solution was found to facilitate the grain growth and results in better crystallization as illustrated in Fig. 3. In addition, the Al^{3+} ions were predominantly expelled to the surface and grain boundaries, which may passivate traps verified by enhanced PLQEs. In general, the improved film quality, such as improved coverage, enhanced crystallinity, and enlarged grain size are also usually accompanied with reduced defects density and improved stability. The existence of bulk film additives in the perovskite film also further interact with perovskites that might passivate defects. In the following Section 4, we further review the progress on the use of bulk film additives for defect reduction/passivation for high quality perovskite films.

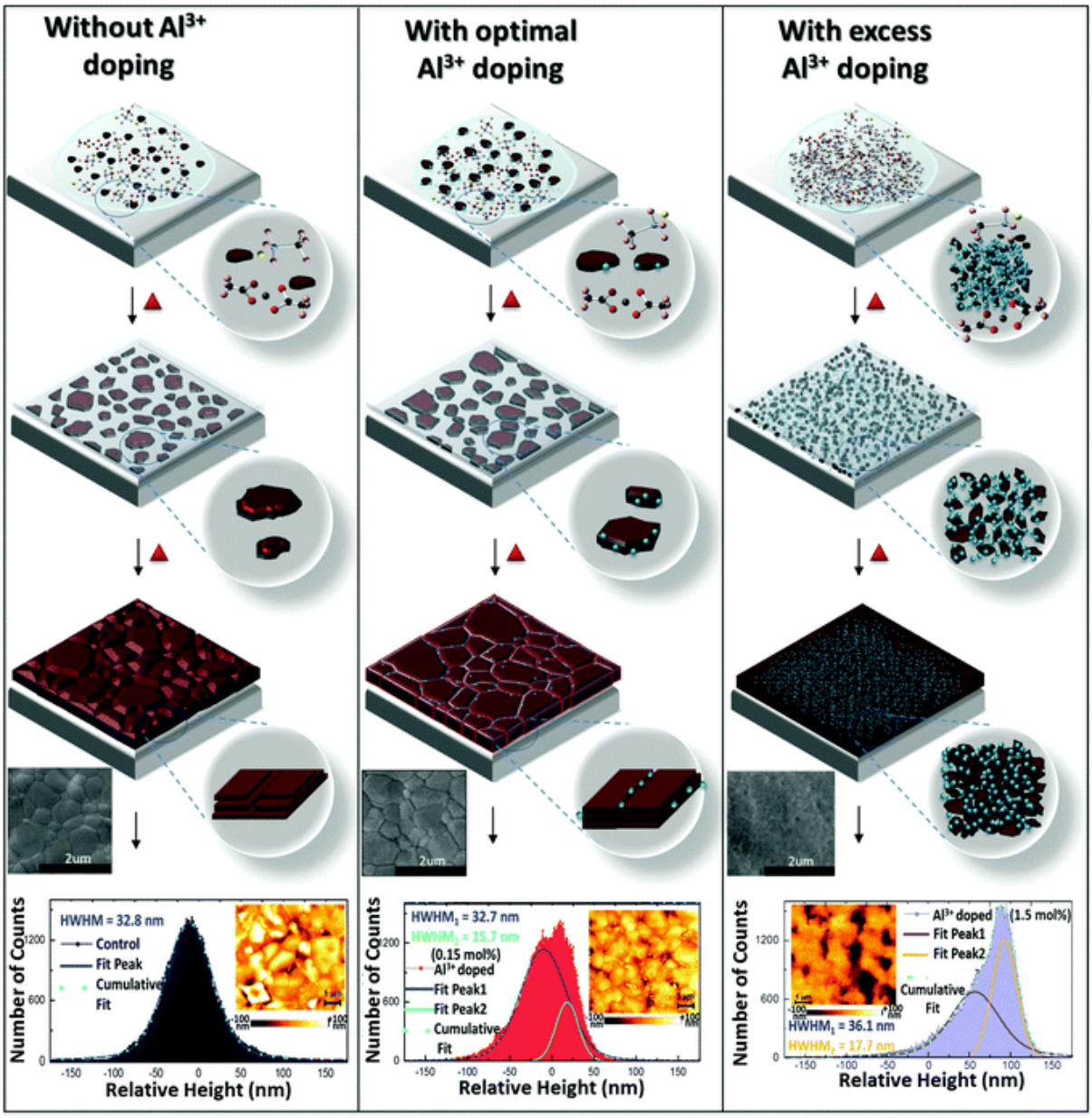

Fig. 3. Schematic diagram of the proposed perovskite polycrystalline thin film growth and influence of the Al^{3+} doping with illustrated C, N, H, O, I, Pb, and Al atoms are indicated by the color of black, blue, pink, red, grey, and cyan respectively; and histograms of the surface topography and the images (insets) from AFM measurements of different samples. Best fits for the histograms are obtained using one and two Voigt distributions, respectively for the control and the optimized sample. The individual distribution components with their HWHM, and the cumulative fits are labelled as in the figure. Reproduced with permission from ref. [90]. Copyright 2016, The Royal Society of Chemistry.

4. Additives for defect density reduction in perovskite films

Crystal structural defects play an important role in the overall performance of perovskite solar cells. Perovskites with an ideal crystal structure have each constituent ion located in its equilibrium site. However, in a real situation, because the perovskite crystal growth is fast and often a subsequent post-annealing step is necessary, the formation of a wide variety of structural defects is unavoidable. These imperfect structural defects could be of a short range (i.e., point defects and impurity atoms/ions) or of a long range (i.e., 1D dislocations, 2D grain boundaries, and 3D precipitates) [19, 91-96]. As the consequence, electronic trap states are generated within the semiconductor band gap limiting performance, lifetime, as well as reproducibility. As a remedy, defect passivation (or defect engineering) has been proposed to heal defects in polycrystalline perovskite thin films. Two approaches have been demonstrated to be effective to heal defects in perovskites, i.e., (i) direct introduction of additives in the perovskite precursor solution and (ii) the post-passivation treatment [97, 98]. In this section, the most commonly employed additives to reduce defects in perovskite films are discussed. Additives suppress defect density not only by forming the coordination chemistry with defects in perovskites, but because additives also improve the film quality (morphology, large grained, high crystallinity, and composition) discussed in Section 3. For example, some additives have been reported to retard the kinetics during crystal growth leading to reduced defect density [28]. When considering upscaling strategies, it is technological challenging to control the kinetics of crystal growth (Section 4.1). In this sense, it is convenient to employ additives into the perovskite precursor ink that can suppress defect density (see Section 4.2).

4.1. Defects in perovskite films

A higher concentration of defects are expected to be formed on the surface and around grain boundaries in perovskite films [99, 100]. The different types of defects are expected to co-exist [19, 96] in perovskite films such as (i) halide-vacancies (e.g., I^- and Br^-) exposing the underlying under-coordinated Pb^{2+} [101-104], (ii) cation-vacancies (e.g., Cs^+, MA^+, FA^+, etc.) [103], (iii) metallic lead (Pb^0) [105, 106], (iv) I_2 (generated as a result of the initial degradation of iodine-containing perovskite films) [107, 108] and (v) anti-site PbI^{3-} defects [109]. Experimentally, defect densities of 3.3×10^{10} cm^{-3} and 5.8×10^9 cm^{-3} were reported for $MAPbI_3$ and $MAPbBr_3$ single crystals, respectively. In comparison, polycrystalline $MAPbI_3$ thin films show a much higher density of defects on the order of 10^{15} cm^{-3} to 10^{17} cm^{-3} [96].

Defects such as under-coordinated Pb^{2+} and Pb^0 become carrier recombination centers, which significantly limit device performance [100, 110]. In addition, vacancy-type defects can cause device instability issues, including ion migration causing current-voltage hysteresis, and device degradation in ambient initialized at defective surfaces and grain boundaries [111]. As comparison, single crystals with a low surface defect density and no grain boundaries demonstrated high stability in air for several years [111]. In another study, thin-sliced $MAPbI_3$ monolithic single crystals (thickness = 20 μm) demonstrated outstanding PCE of 21.09% and FF up to 84.3% [112]. These studies show the superior performance of single crystal perovskite based solar cells. However, at this stage it is still technologically challenging to upscale perovskite single crystal based solar cells at low cost [113-117].

4.2. Defect passivation using additives in perovskite films

As discussed in Section 2, it is important to develop upscaling strategies for large area perovskite thin film coating processes [5, 15-17]. Incorporation of a small amount of surfactants [18], Cl^- ions [22-24], DIO [28] and H_2O [26, 27] was proposed as an effective method to reduce defect densities in large area perovskite films and compatible with upscalable coating techniques (e.g., doctor blading). Huang and co-workers [18] demonstrated that ~20 ppm of L-α-phosphatidylcholine surfactant added into the $MAPbI_3$/DMF precursor solution led to improvement in the film quality of blade-coated perovskite films. A PCE of 14.6% was reported for their solar modules with an aperture area of 57.2 cm^2. Surfactants have two mechanisms in decreasing the defect density: (i) improvement of film coverage and morphology by enhancing the adhesion of the perovskite film to hydrophobic substrates (e.g., PTAA or P3HT) and (ii) passivation of perovskite defects by functional groups (Lewis acid or Lewis base coordination) [110]. Cl^- ions from $PbCl_2$ and/or MACl precursors added into the $MAPbI_3$ solution were shown to enhance both the device performance and stability, in addition to the compatibility to be incorporated in the upscaling process. Cl^- ions suppress the defect density by (i) controlling the crystallization rate to enhance the grain size; (ii) Cl^- ions passivate undercoordinated Pb^{2+} defects present at grain boundaries and the perovskite/TiO_2 interface (in the case of the n-i-p structure); and (iii) Cl^- ions mitigate the reaction between I^- and the top electrode (e.g., making the silver electrode to silver iodide) [22, 43, 118]. It is generally believed that the vast majority of Cl^- in the solution-processed perovskite films are sublimated (e.g., as MACl) [21, 119] during the thermal annealing step. A maximal chloride to iodide ratio of <4 at% is reported as the upper bound of the Cl^- amount that can be incorporated into the

$MAPbI_3$ films. Cl^- ions remaining in the final films are mainly incorporated at grain boundaries and at the $MAPbI_3/TiO_2$ interfaces and demonstrated to have the defect healing (passivation) functionality [21, 120, 121].

Several other inorganic cationic passivation materials such as K^+, Al^{3+}, Cs^+, and Rb^+ were also reported to passivate defects (undercoordinated I^-, antisite PbI_3^-, and MA^+ vacancies) present at grain boundaries and perovskite surfaces, in addition to bulk defects [31, 32, 85, 122-125]. Recently, incorporation of K^+ in perovskite films were shown to decrease (i) photocurrent hysteresis [31, 32] and (ii) enhance the internal photoluminescence quantum efficiency (PLQE) over 95% (Fig. 4) [33]. Stranks and co-workers proposed that K^+ in $Cs_{0.06}FA_{0.79}MA_{0.15}Pb(I_{0.85}Br_{0.15})_3$ perovskite films accumulates at the grain boundaries and surfaces passivating the undercoordinated I^- and Br^- halides (Fig. 4a). Defect passivation at grain boundaries and surfaces led to enhancement in external PLQE (Fig. 4b) and hysteresis free perovskite-based solar cells (Fig. 4c). Experimental evidence for the incorporation of K^+ into the $FA_{0.85}MA_{0.15}Pb(I_{0.85}Br_{0.15})_3$ crystal lattice was proposed by Segawa and co-workers [31]. Park and co-workers conducted a systematic study to investigate the influences of alkali metal ions on the hysteresis phenomena on $(FAPbI_3)_{0.875}(CsPbBr_3)_{0.125}$ based perovskite solar cells (Fig. 4d, e). K^+ was shown to effectively suppress hysteresis. On the basis of DFT calculations, the authors proposed that K^+ are favorably incorporated into the interstitial sites of the perovskite crystal structure (Fig. 4f), which blocks the iodine Frenkel pair defect formation and suppresses ion migration [32]. Although K^+, Rb^+, Cu^+, and Ag^+ were reported as effective in passivating defects and suppressing ion migration, the mechanism of the interactions is yet to be further studied [84, 126-128]. Furthermore, incorporation of the abovementioned monovalent cations warrants further investigation in terms of upscaling strategies.

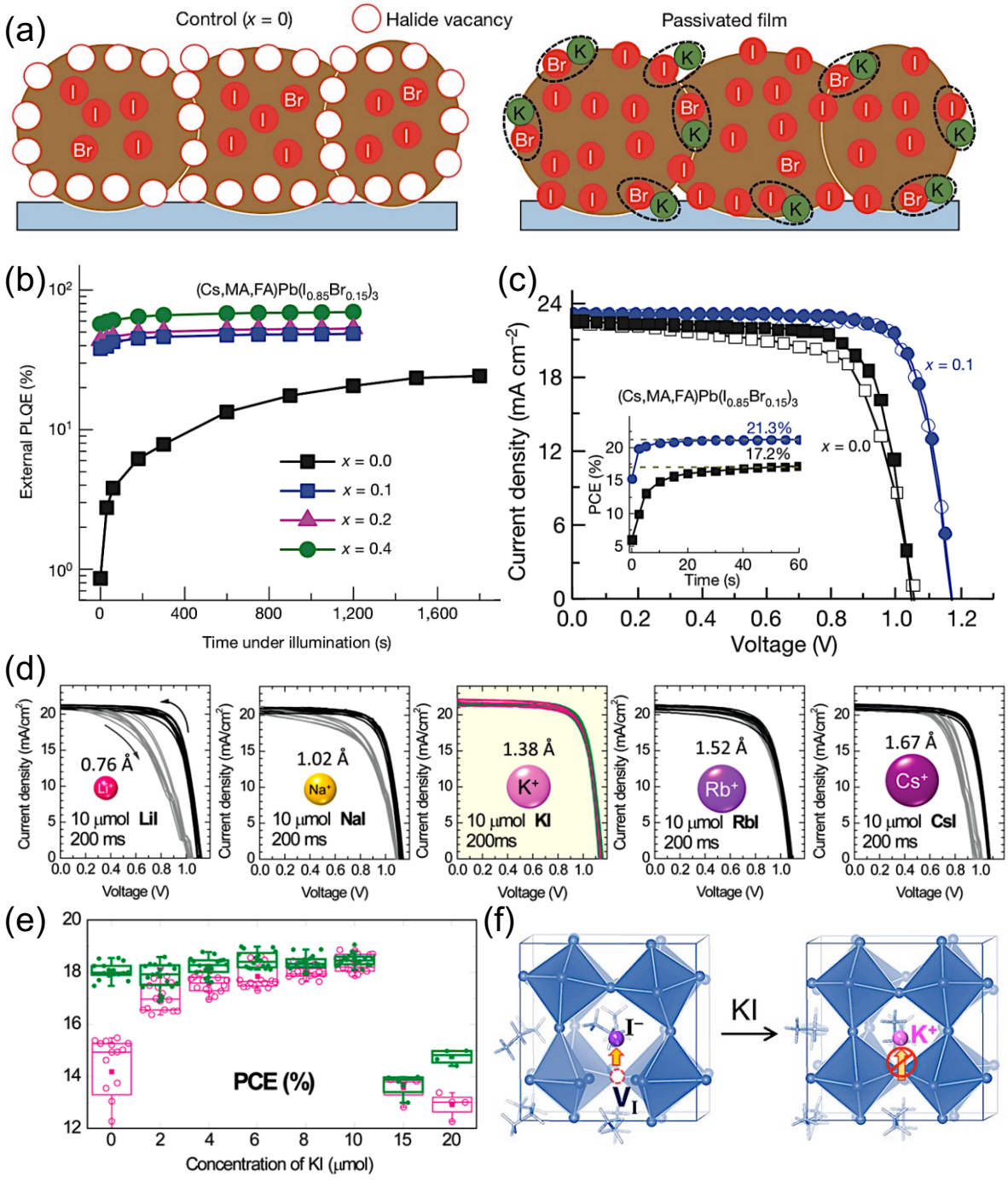

Fig. 4. (a) Proposed schematic of K^+ incorporation overcoming the halide-vacancy (Control), in which the excess of halides (I^- and Br^-) can be immobilized through complexation with K^+ at grain boundaries and surfaces. (b) PLQE time evolution of perovskites illuminated with a 532 nm laser (60 mW cm^{-2}) in ambient atmosphere. (c) Forward (open symbols) and reverse (closed symbols) J–V curves of perovskite absorbers without (x = 0) and with (x = 0.1) passivation, measured under AM1.5, 100 mW cm^{-2}. Reprinted with permission from ref. [33]. Copyright 2018, Springer Nature. (d) J-V curves of $(FAPbI_3)_{0.875}(CsPbBr_3)_{0.125}$ doped with 10 μmol of LiI, NaI, KI, RbI and CsI, measured at reverse and forward scans under AM 1.5G one

sun illumination (100 mW/cm^2). (e) Extracted PCEs from reverse (green) and forward (pink) scans as a function of KI concentration. (f) Schematic view of $MAPbI_3$ perovskite structure with I Frenkel defect. K^+ is proposed to occupy the interstitial sites within the perovskite lattice suppressing I Frenkel defect. Reprinted with permission from ref. [32]. Copyright 2018, American Chemical Society.

Small organic passivation molecules such as AVA [102], 2,3,5,6-Tetrafluoro-7,7,8,8-tetracyanoquinodimethane (F4TCNQ) [129], pyridine [130], PCBM [109], guanidinium [67, 131], and other passivation molecules with Lewis acid or base functionality [94, 132] were successfully applied into the perovskite precursor solutions to passivate the different types of defects. However, most of these passivation molecules can only passivate one type of defects. Currently, there is a trend in employing passivating molecules with the dual function of Lewis base and Lewis acid to passivate the positively and negatively charged type defects simultaneously [96]. Huang and co-workers [103] employed 3-(decyldimethylammonio)-propane-sulfonate inner salt (DPSI), a sulfonic zwitterion, which contains both a positively charged quaternary ammonium group and a negatively charged sulfonic group. The coordination of sulfonic group (S=O) of DPSI to $MAPbI_3$ by the donation of their lone unpaired electron to the empty orbitals of Pb^{2+} was proposed. Alternatively, Zhu, Gratzel, and co-workers [104] reported employing bis-PCBM as the Lewis acid and N-(4-bromophenyl)thiourea (BrPh-ThR) as the Lewis base. The combination of these two passivating molecules shows the synergistic effect of passivating both the positively charged under-coordinated Pb^{2+} and the negatively charged PbX^{3-} antisite defects. These examples show the importance of employing additives for enhancing performance by defect healing. In the next section, we discuss the stability of the passivating agents with the perovskites, which has implications on the long-term operational stability.

5. Additives for enhancing perovskite film stability

A large number of strategies have been developed for enhancing the long-term operational stability in lab-scale small area PSCs and solar modules. As already highlighted in several review articles, the perovskite layer need be resilient to moisture, oxygen, light, bias, and elevated temperatures under realistic solar cell operation conditions [133-136]. It has been recently proposed that the stability of perovskite films are associated with the presence of defects: (i) defective grain boundaries with a high density of trapped charges accelerate moisture-induced degradation [111]; (ii) trapped charges at grain boundaries and surfaces

promote formation of volatile CH_3NH_2 and CH_3I upon light exposure, leading to irreversible degradation [105, 137]; (iii) trapped charges in the perovskite layer induces formation of oxygen peroxides (O_2^-) that accelerates degradation [138]. As discussed in Section 5.1, the density of trap states in the perovskite layer can be suppressed by additives that passivate defects. Considering the long-term stability, it is important to examine the coordination strength between defect sites in the perovskite layer and the additive (Section 5.1). The shelf lifetime of the perovskite precursor solution is also an important consideration for upscaling strategies (Section 5.2).

5.1 Additives for improving stability of perovskite films

Defects such as halide vacancies and under-coordinated Pb^{2+} were reported to show enhanced reactivity with H_2O and O_2. Therefore, it is necessary to rationally design and synthesize the additives with one end that can attach to defects in the perovskite layer and the other end with a hydrophobic functional group [139-141]. Huang and co-workers employed a series of bilateral alkylamine (BAA) additives of 1,3-diaminopropane (DAP), 1,6-diaminohexane (DAH), and 1,8-diaminooctane (DAO) in the perovskite precursor for blade coating (Fig. 5) [141]. The $–NH_2$ tails at both ends of BAA additives coordinate with under-coordinated Pb^{2+} or occupy cation-site vacancies leading to enhanced Voc (the optical bandgap of the Cs/FA/MA mixed-cation perovskite was 1.51 eV and has a high Voc of 1.16 V, corresponding to a low Voc deficit of 0.35 V). The exposed alkyl chain is hydrophobic and forms a barrier at grain boundaries and surfaces protecting perovskite against moisture (Fig. 5). In addition, the employment of BAA additives was demonstrated to be compatible for upscaling processes with doctor-blade coating (Fig. 5). The device structure of ITO/PTAA/$MAPbI_3$ + DAP/C60/BCP/Cu achieved a PCE of 20% (aperture, 1.1 cm^2), and retained 90% of its initial PCE under operational stability testing for >500 h [141].

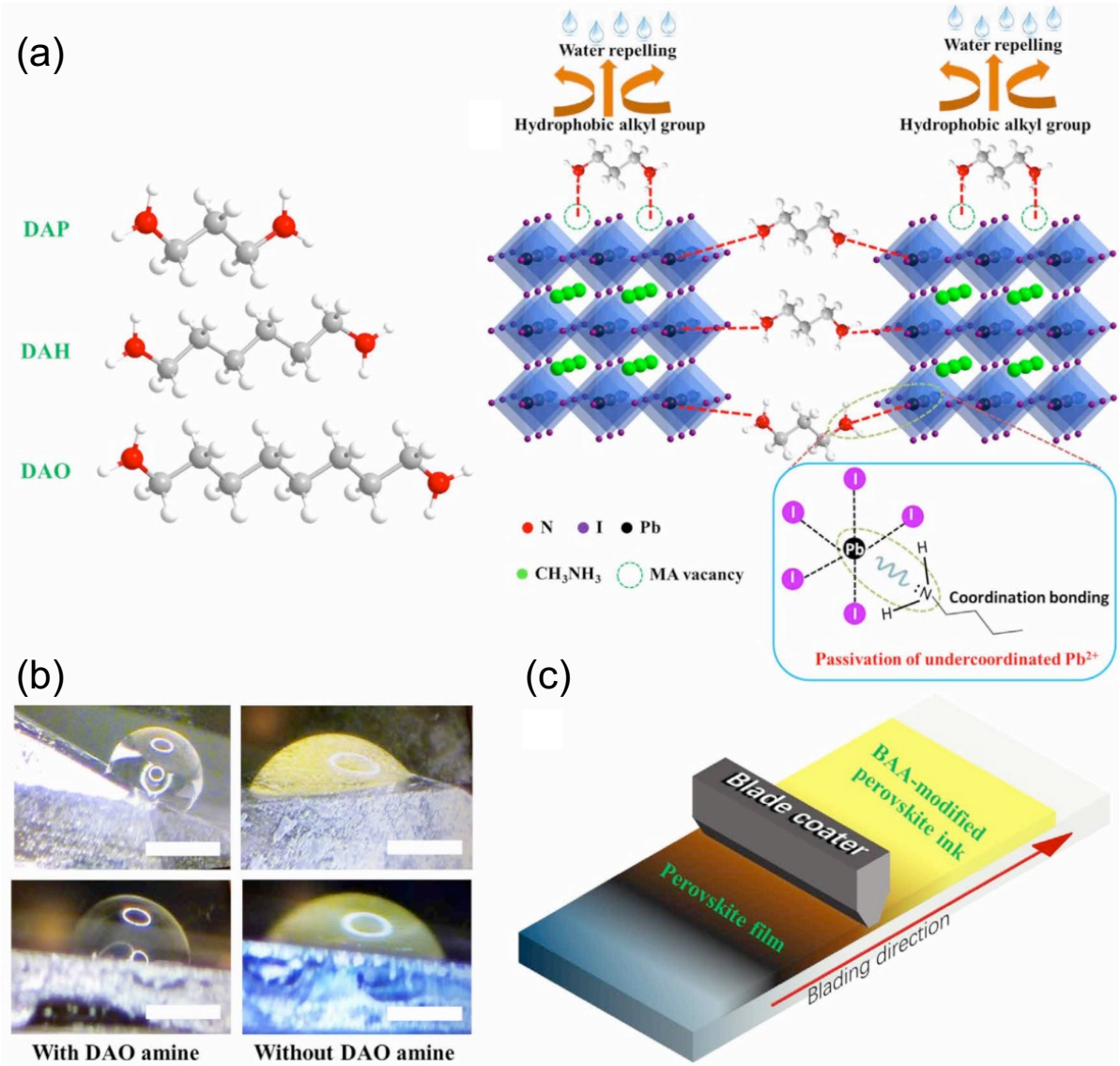

Fig. 5. (a) The series of bilateral alkylamine (BAA) additives of DAP, DAH, and DAO are shown to be efficient to passivate defects and enhance water repellence. (b) Contact angle measurements of a water droplet on $MAPbI_3$ single crystals (top row) and $MAPbI_3$ thin films (bottom row) with or without the BAA additive. Scale bars correspond to 5 cm. (c) Compatibility with upscaling using blade-coating process is demonstrated. Reprinted with permission from ref. [141]. Copyright 2019, American Association for the Advancement of Science (AAAS).

The chemical stability of passivating molecules is an important consideration for long-term stability. It is desirable that the passivating molecules are strongly anchored to the defect sites in perovskites. However, it has been reported that some passivating molecules can be washed away easily with common solvents (e.g., isopropanol [142], chlorobenzene [143], etc.). Wu,

Zhu, and co-workers showed that the use of 2-mercaptopyridine (2-MP), a bidentate molecule, increases the anchoring strength improving passivation efficacy and stability simultaneously [143]. Compared with the monodentate counterparts of pyridine and *p*-toluenethiol where the coordination with Pb^{2+} can be broken easily due to low binding strength, the passivation by 2-MP of the $CH_3NH_3PbI_3$ film led to enhanced tolerance to chlorobenzene washing and vacuum heating. Desorption of organic A^+ cations has been pointed out to contribute to the permanent degradation during solar cell operation [105]. A few strategies have been reported to immobilize the A^+ cations. Qiao, Li, and co-workers have proposed that rubrene interacts strongly with MA^+ cations (calculated interaction energy of ~1.5 eV). This binding energy is sufficient to immobilize the organic cations, enhance perovskite surface stability, and reduce ion migration [144]. Polymers are also widely applied in perovskites to reduce defects and enhance thermal- and photo-stability. Polymer cross-linking engineering starts to gain attention because of its ability to immobilize surface atoms/ions at grain boundaries and enhance material stability [145, 146]. Fang and co-workers employed cross-linkable monomers of trimethylolpropane triacrylate (TMTA) mixed into the $MAPbI_3$ perovskite precursor solution [146]. During perovskite crystallization, TMTA is expelled to grain boundaries without interruption of the perovskite crystal growth. The carbonyl group in TMTA interacts with PbI_2 leading to chemical anchoring to grain boundaries and further passivation of defects. The alkenyl groups in TMTA allow cross-linking polymerization upon annealing. TMTA-containing $MAPbI_3$-based PSCs showed an outstanding long-term stability retaining 80% of its initial efficiency after continuous power output under maximum power point tracking for 400 h [146].

5.2 Stability issues in perovskite precursor solutions

The influence of perovskite precursor aging on the perovskite film crystallinity, morphology, and chemical composition and the overall device performance is an important consideration [13, 147-149]. Lu and co-workers studied the properties of $MA_{0.17}FA_{0.83}Pb(I_{0.83}Br_{0.17})_3$ perovskite films from the precursor solution aged at different times (Fig. 6) [147]. The formation of the δ-phase perovskite film is observed when using the precursor solution aged for 12 days (Fig. 6). The incorporation of 3,9-bis(2-methylene-(3-(1,1-dicyanomethylene)-indanone))-5,5,11,11-tetrakis(5-hexylthienyl)-dithieno[2,3-d:2',3'-d']-s-indaceno[1,2-b:5,6-b'] dithiophene (ITIC-Th) suppress effectively the unwanted δ-phase formation made from the long-time aged (96 days) precursor solution (Fig. 6). Dou, van Hest,

and co-workers studied the mechanisms of degradation in the $Cs_{0.05}(MA_{0.17}FA_{0.83})_{0.95}Pb(I_{0.83}Br_{0.17})_3$ perovskite precursor solution [148]. Despite the precursor solution is stored under inert conditions, the unavoidable trace amount of H_2O lead to hydrolysis of DMF producing dimethylammonium formate. Dimethylammonium cations (DMA^+) can be incorporated into the perovskite films and affect the optoelectronic properties of the spin-coated films and devices [148]. On the basis of the review topics in this section, strategies to suppress the defect density and the precursor solution aging time are important consideration that affect the long-term device stability in perovskite solar modules.

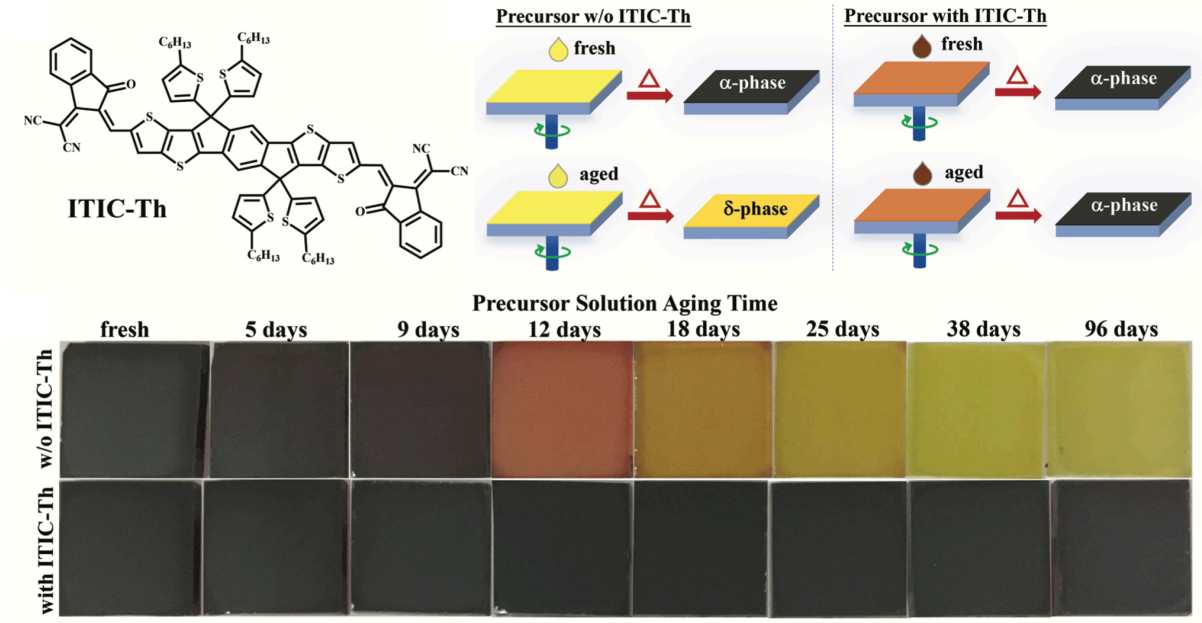

Fig. 6. Schematic of perovskite films fabricated from the fresh and aged precursor solutions without and with ITIC-Th. A series of photographs of films fabricated from perovskite precursor solutions aged for different amount of time without and with ITIC-Th are shown. Reprinted with permission from ref. [147]. Copyright 2018, WILEY-VCH Verlag GmbH & Co. KGaA, Weinheim.

6. Conclusions and perspectives

In this review article, we discuss bulk film additives in metal halide perovskite films and their applications in PSCs. To realize practical applications, large area PSCs need overcome the existing bottlenecks, such as scalability, long-term stability, and efficiency. As the film quality of large area perovskite films limits their efficiency and stability, it is critical to control the perovskite film quality. We first review the progress on large scale PSCs that using additives during perovskite film fabrication. The additives interact with perovskite during

the film formation and affect the film morphology, defects density, and film stability and thus influence device performance and stability.

As most of the successful demonstration of additive engineering strategy are based on small size PSCs, we give a comprehensive review of the progress on additive engineering. The detailed discussion reveals their multiple effects on the perovskite film quality during and after the film formation. During the film formation process, the additives interact with Pb^{2+} ions via coordination interaction or organic ammonium with hydrogen bond interaction to form intermediate or complex. These interactions largely affect the crystal growth kinetics that govern the film growth process. A fine selection of additives is able to tune the morphology of resulting film morphology. The improved film quality, such as improved coverage, enhanced crystallinity, and enlarged grain size are also usually accompanied with reduced defects density and improved stability.

Defects such as halide vacancies and under-coordinated Pb^{2+} present majorly at grain boundaries and surfaces of perovskites. They were associated as charge recombination sites that cause electric loss and reaction with H_2O and O_2 causing film degradation followed by hampering in device long term stability. After film formation, the additives are kept at a certain concentration in the final perovskite bulk films as foreign species. Although these additives are not the component of the perovskite structure, they locate at the grain boundaries and can further interact with the defects in perovskite films via Lewis acid-base interaction or hydrogen bond interaction. These interactions also lead to defects passivation and stability improvement and benefits the device performance and stability.

Inspired by the accumulated successful experience of using additive in PSC fabrication, additive engineering has a great chance to further enable the achievement of high-throughput manufacturing of large-scale, high efficiency, and stable perovskite solar modules. Although lots of additives have been employed in PSCs, more research efforts are needed to develop new additives to further extend the advantages of additive engineering. In addition, the understanding of how the additives affect the film formation, defects reduction/passivation and stability enhancement need further exploration. In particular, some *in situ* characterizations can reveal the sophisticated interaction of additives with perovskites during and after film formation, which can help provide a full map of the mechanism of engineering. This information will not only improve the understanding of additive engineering, but also prove helpful guidance for the selection or exploration of new additives.

Acknowledgements

This work was supported by funding from the Energy Materials and Surface Sciences Unit of the Okinawa Institute of Science and Technology Graduate University, the OIST R&D Cluster Research Program, the OIST Proof of Concept (POC) Program, and JSPS KAKENHI Grant Number JP18K05266.

References

[1] A. Kojima, K. Teshima, Y. Shirai, T. Miyasaka, J. Am. Chem. Soc. 131 (2009) 6050-6051.

[2] H.-S. Kim, C.-R. Lee, J.-H. Im, K.-B. Lee, T. Moehl, A. Marchioro, S.-J. Moon, R. Humphry-Baker, J.-H. Yum, J.E. Moser, M. Grätzel, N.-G. Park, Sci. Rep. 2 (2012) 591.

[3] M.M. Lee, J. Teuscher, T. Miyasaka, T.N. Murakami, H.J. Snaith, Science 338 (2012) 643-647.

[4] Q. Jiang, Y. Zhao, X. Zhang, X. Yang, Y. Chen, Z. Chu, Q. Ye, X. Li, Z. Yin, J. You, Nat. Photon. 13 (2019) 460-466.

[5] Y. Rong, Y. Hu, A. Mei, H. Tan, M.I. Saidaminov, S.I. Seok, M.D. McGehee, E.H. Sargent, H. Han, Science 361 (2018) eaat8235.

[6] N.-G. Park, M. Grätzel, T. Miyasaka, K. Zhu, K. Emery, Nat. Energy 1 (2016) 16152.

[7] (20190802).

[8] L. Qiu, S. He, L.K. Ono, S. Liu, Y.B. Qi, ACS Energy Lett. (2019) 2147-2167.

[9] J.-P. Correa-Baena, M. Saliba, T. Buonassisi, M. Grätzel, A. Abate, W. Tress, A. Hagfeldt, Science 358 (2017) 739-744.

[10] W.A. Dunlap-Shohl, Y. Zhou, N.P. Padture, D.B. Mitzi, Chem. Rev. 119 (2019) 3193-3295.

[11] F. Huang, M. Li, P. Siffalovic, G. Cao, J. Tian, Energy Environ. Sci. 12 (2019) 518-549.

[12] T.-B. Song, Q. Chen, H. Zhou, C. Jiang, H.-H. Wang, Y. Yang, Y. Liu, J. You, Y. Yang, J. Mater. Chem. A 3 (2015) 9032-9050.

[13] M. Jung, S.-G. Ji, G. Kim, S.I. Seok, Chem. Soc. Rev. 48 (2019) 2011-2038.

[14] Y. Jiang, M. Remeika, Z. Hu, E.J. Juarez-Perez, L. Qiu, Z. Liu, T. Kim, L.K. Ono, D.-Y. Son, Z. Hawash, M.R. Leyden, Z. Wu, L. Meng, J. Hu, Y.B. Qi, Adv. Energy Mater. 9 (2019) 1803047.

[15] Z. Li, T.R. Klein, D.H. Kim, M. Yang, J.J. Berry, M.F.A.M. van Hest, K. Zhu, Nat. Rev. Mater. 3 (2018) 18017.

[16] J.-W. Lee, D.-K. Lee, D.-N. Jeong, N.-G. Park, Adv. Funct. Mater. (2018) 1807047.

[17] D.H. Kim, J.B. Whitaker, Z. Li, M.F.A.M. van Hest, K. Zhu, Joule 2 (2018) 1437-1451.

[18] Y. Deng, X. Zheng, Y. Bai, Q. Wang, J. Zhao, J. Huang, Nat. Energy 3 (2018) 560-566.
[19] B. Chen, P.N. Rudd, S. Yang, Y. Yuan, J. Huang, Chem. Soc. Rev. 48 (2019) 3842-3867.
[20] T. Li, Y. Pan, Z. Wang, Y. Xia, Y. Chen, W. Huang, J. Mater. Chem. A 5 (2017) 12602-12652.
[21] L.K. Ono, E.J. Juarez-Perez, Y.B. Qi, ACS Appl. Mater. Interfaces 9 (2017) 30197-30246.
[22] H.C. Liao, P. Guo, C.P. Hsu, M. Lin, B. Wang, L. Zeng, W. Huang, C.M.M. Soe, W.F. Su, M.J. Bedzyk, M.R. Wasielewski, A. Facchetti, R.P.H. Chang, M.G. Kanatzidis, T.J. Marks, Adv. Energy Mater. 7 (2017) 1601660.
[23] M. Yang, Z. Li, M.O. Reese, O.G. Reid, D.H. Kim, S. Siol, T.R. Klein, Y. Yan, J.J. Berry, M.F.A.M. van Hest, K. Zhu, Nat. Energy 2 (2017) 17038.
[24] Z. Liu, L. Qiu, E.J. Juarez-Perez, Z. Hawash, T. Kim, Y. Jiang, Z. Wu, S.R. Raga, L.K. Ono, S.F. Liu, Y.B. Qi, Nat. Commun. 9 (2018) 3880.
[25] G. Niu, X. Guo, L. Wang, J. Mater. Chem. A 3 (2015) 8970-8980.
[26] J. Huang, S. Tan, P.D. Lund, H. Zhou, Energy Environ. Sci. 10 (2017) 2284-2311.
[27] C.-H. Chiang, M.K. Nazeeruddin, M. Gratzel, C.-G. Wu, Energy Environ. Sci. 10 (2017) 808-817
[28] P.-W. Liang, C.-Y. Liao, C.-C. Chueh, F. Zuo, S.T. Williams, X.-K. Xin, J. Lin, A.K.Y. Jen, Adv. Mater. 26 (2014) 3748-3754.
[29] G. Fu, L. Hou, Y. Wang, X. Liu, J. Wang, H. Li, Y. Cui, D. Liu, X. Li, S. Yang, Sol. Energy Mater. Sol. Cells 165 (2017) 36-44.
[30] T. Bu, X. Liu, Y. Zhou, J. Yi, X. Huang, L. Luo, J. Xiao, Z. Ku, Y. Peng, F. Huang, Y.-B. Cheng, J. Zhong, Energy Environ. Sci. 10 (2017) 2509-2515.
[31] Z. Tang, T. Bessho, F. Awai, T. Kinoshita, M.M. Maitani, R. Jono, T.N. Murakami, H. Wang, T. Kubo, S. Uchida, H. Segawa, Sci. Rep. 7 (2017) 12183.
[32] D.-Y. Son, S.-G. Kim, J.-Y. Seo, S.-H. Lee, H. Shin, D. Lee, N.-G. Park, J. Am. Chem. Soc. 140 (2018) 1358-1364.
[33] M. Abdi-Jalebi, Z. Andaji-Garmaroudi, S. Cacovich, C. Stavrakas, B. Philippe, J.M. Richter, M. Alsari, E.P. Booker, E.M. Hutter, A.J. Pearson, S. Lilliu, T.J. Savenije, H. Rensmo, G. Divitini, C. Ducati, R.H. Friend, S.D. Stranks, Nature 555 (2018) 497.
[34] M.R. Leyden, L.K. Ono, S.R. Raga, Y. Kato, S. Wang, Y.B. Qi, J. Mater. Chem. A 2 (2014) 18742-18745.
[35] L.K. Ono, M.R. Leyden, S. Wang, Y.B. Qi, J. Mater. Chem. A 4 (2016) 6693-6713.
[36] L. Qiu, S. He, Y. Jiang, D.-Y. Son, L.K. Ono, Z. Liu, T. Kim, T. Bouloumis, S. Kazaoui, Y.B. Qi, J. Mater. Chem. A 7 (2019) 6920-6929.

[37] L. Luo, Y. Zhang, N. Chai, X. Deng, J. Zhong, F. Huang, Y. Peng, Y.-B. Cheng, Z. Ku, J. Mater. Chem. A 6 (2018) 21143-21148.
[38] A. Priyadarshi, L.J. Haur, P. Murray, D. Fu, S. Kulkarni, G. Xing, T.C. Sum, N. Mathews, S.G. Mhaisalkar, Energy Environ. Sci. 9 (2016) 3687-3692.
[39] Y. Hu, S. Si, A. Mei, Y. Rong, H. Liu, X. Li, H. Han, Solar RRL 1 (2017) 1600019.
[40] G. Grancini, C. Roldán-Carmona, I. Zimmermann, E. Mosconi, X. Lee, D. Martineau, S. Narbey, F. Oswald, F. De Angelis, M. Graetzel, M.K. Nazeeruddin, Nat. Commun. 8 (2017) 15684.
[41] Y. Zhao, K. Zhu, J. Phys. Chem. Lett. 5 (2014) 4175-4186.
[42] Y. Zhou, O.S. Game, S. Pang, N.P. Padture, J. Phys. Chem. Lett. 6 (2015) 4827-4839.
[43] K. Odysseas Kosmatos, L. Theofylaktos, E. Giannakaki, D. Deligiannis, M. Konstantakou, T. Stergiopoulos, Energy Environ. Mater. 2 (2019) 79-92.
[44] Y. Zhao, K. Zhu, J. Phys. Chem. C 118 (2014) 9412-9418.
[45] D. Liu, C. Li, C. Zhang, Z. Wang, H. Zhang, J. Tian, S. Pang, RSC Adv. 7 (2017) 51944-51949.
[46] Q. Chen, H. Zhou, Y. Fang, A.Z. Stieg, T.-B. Song, H.-H. Wang, X. Xu, Y. Liu, S. Lu, J. You, P. Sun, J. McKay, M.S. Goorsky, Y. Yang, Nat. Commun. 6 (2015) 7269.
[47] B. Li, M. Li, C. Fei, G. Cao, J. Tian, J. Mater. Chem. A 5 (2017) 24168-24177.
[48] M. Ralaiarisoa, Y. Busby, J. Frisch, I. Salzmann, J.-J. Pireaux, N. Koch, Phys. Chem. Chem. Phys. 19 (2017) 828-836.
[49] J.H. Heo, M.H. Lee, M.H. Jang, S.H. Im, J. Mater. Chem. A 4 (2016) 17636-17642.
[50] N. Yantara, F. Yanan, C. Shi, H.A. Dewi, P.P. Boix, S.G. Mhaisalkar, N. Mathews, Chem. Mater. 27 (2015) 2309-2314.
[51] S. Colella, E. Mosconi, G. Pellegrino, A. Alberti, V.L.P. Guerra, S. Masi, A. Listorti, A. Rizzo, G.G. Condorelli, F. De Angelis, G. Gigli, J. Phys. Chem. Lett. 5 (2014) 3532-3538.
[52] H. Yu, F. Wang, F. Xie, W. Li, J. Chen, N. Zhao, Adv. Funct. Mater. 24 (2014) 7102-7108.
[53] D.E. Starr, G. Sadoughi, E. Handick, R.G. Wilks, J.H. Alsmeier, L. Kohler, M. Gorgoi, H.J. Snaith, M. Bar, Energy Environ. Sci. 8 (2015) 1609-1615.
[54] E.L. Unger, A.R. Bowring, C.J. Tassone, V.L. Pool, A. Gold-Parker, R. Cheacharoen, K.H. Stone, E.T. Hoke, M.F. Toney, M.D. McGehee, Chem. Mater. 26 (2014) 7158-7165.
[55] H. Zhang, Q. Liao, X. Wang, K. Hu, J. Yao, H. Fu, Small 12 (2016) 3780-3787.
[56] V.L. Pool, A. Gold-Parker, M.D. McGehee, M.F. Toney, Chem. Mater. 27 (2015) 7240-7243.

[57] J. Chae, Q. Dong, J. Huang, A. Centrone, Nano Lett. 15 (2015) 8114-8121.
[58] Y. Chen, T. Chen, L. Dai, Adv. Mater. 27 (2015) 1053-1059.
[59] L. Cojocaru, S. Uchida, A.K. Jena, T. Miyasaka, J. Nakazaki, T. Kubo, H. Segawa, Chem. Lett. 44 (2015) 1089-1091.
[60] Z. Wang, Y. Zhou, S. Pang, Z. Xiao, J. Zhang, W. Chai, H. Xu, Z. Liu, N.P. Padture, G. Cui, Chem. Mater. 27 (2015) 7149-7155.
[61] M. Kim, G.-H. Kim, T.K. Lee, I.W. Choi, H.W. Choi, Y. Jo, Y.J. Yoon, J.W. Kim, J. Lee, D. Huh, H. Lee, S.K. Kwak, J.Y. Kim, D.S. Kim, Joule (2019) DOI: 10.1016/j.joule.2019.06.014.
[62] S. Tang, Y. Deng, X. Zheng, Y. Bai, Y. Fang, Q. Dong, H. Wei, J. Huang, Adv. Energy Mater. 7 (2017) 1700302.
[63] C. Li, Y. Zhou, L. Wang, Y. Chang, Y. Zong, L. Etgar, G. Cui, N.P. Padture, S. Pang, Angew. Chem. Int. Ed. 129 (2017) 7782-7786.
[64] C. Zuo, L. Ding, Nanoscale 6 (2014) 9935-9938.
[65] Y. Rong, X. Hou, Y. Hu, A. Mei, L. Liu, P. Wang, H. Han, Nat. Commun. 8 (2017) 14555.
[66] G. Tong, X. Lan, Z. Song, G. Li, H. Li, L. Yu, J. Xu, Y. Jiang, Y. Sheng, Y. Shi, K. Chen, Mater. Today Energy 5 (2017) 173-180.
[67] N. De Marco, H. Zhou, Q. Chen, P. Sun, Z. Liu, L. Meng, E.-P. Yao, Y. Liu, A. Schiffer, Y. Yang, Nano Lett. 16 (2016) 1009-1016.
[68] Q. Han, Y. Bai, J. Liu, K.-z. Du, T. Li, D. Ji, Y. Zhou, C. Cao, D. Shin, J. Ding, A.D. Franklin, J.T. Glass, J. Hu, M.J. Therien, J. Liu, D.B. Mitzi, Energy Environ. Sci. 10 (2017) 2365-2371.
[69] S. Yang, W. Liu, L. Zuo, X. Zhang, T. Ye, J. Chen, C.-Z. Li, G. Wu, H. Chen, J. Mater. Chem. A 4 (2016) 9430-9436.
[70] H. Dong, Z. Wu, J. Xi, X. Xu, L. Zuo, T. Lei, X. Zhao, L. Zhang, X. Hou, A.K.Y. Jen, Adv. Funct. Mater. (2017) 1704836.
[71] Y. Xia, C. Ran, Y. Chen, Q. Li, N. Jiang, C.-Z. Li, Y. Pan, T. Li, J. Wang, W. Huang, J. Mater. Chem. A 5 (2017) 3193-3202.
[72] Q. Wu, P. Zhou, W. Zhou, X. Wei, T. Chen, S. Yang, ACS Appl. Mater. Interfaces 8 (2016) 15333-15340.
[73] C.-Y. Chang, C.-Y. Chu, Y.-C. Huang, C.-W. Huang, S.-Y. Chang, C.-A. Chen, C.-Y. Chao, W.-F. Su, ACS Appl. Mater. Interfaces 7 (2015) 4955-4961.
[74] Y. Zhao, J. Wei, H. Li, Y. Yan, W. Zhou, D. Yu, Q. Zhao, Nat. Commun. 7 (2016) 10228.

[75] D. Bi, C. Yi, J. Luo, J.-D. Décoppet, F. Zhang, Shaik M. Zakeeruddin, X. Li, A. Hagfeldt, M. Grätzel, Nat. Energy 1 (2016) 16142.
[76] N. Tripathi, Y. Shirai, M. Yanagida, A. Karen, K. Miyano, ACS Appl. Mater. Interfaces 8 (2016) 4644-4650.
[77] Y. Guo, K. Shoyama, W. Sato, E. Nakamura, Adv. Energy Mater. 6 (2016) 1502317.
[78] Y. Wang, J. Luo, R. Nie, X. Deng, Energy Technol. 4 (2016) 473-478.
[79] K.M. Boopathi, M. Ramesh, T.-Y. Huang, W. Budiawan, M.Y. Lin, C.-H. Lee, K.-C. Ho, C.W. Chu, J. Mater. Chem. A 4 (2016) 1591-1597.
[80] S. Bag, M.F. Durstock, ACS Appl. Mater. Interfaces 8 (2016) 5053-5057.
[81] N. Li, S. Tao, Y. Chen, X. Niu, C.K. Onwudinanti, C. Hu, Z. Qiu, Z. Xu, G. Zheng, L. Wang, Y. Zhang, L. Li, H. Liu, Y. Lun, J. Hong, X. Wang, Y. Liu, H. Xie, Y. Gao, Y. Bai, S. Yang, G. Brocks, Q. Chen, H. Zhou, Nat. Energy 4 (2019) 408-415.
[82] M. Saliba, T. Matsui, K. Domanski, J.-Y. Seo, A. Ummadisingu, S.M. Zakeeruddin, J.-P. Correa-Baena, W.R. Tress, A. Abate, A. Hagfeldt, M. Grätzel, Science 354 (2016) 206-209.
[83] G. Zheng, C. Zhu, J. Ma, X. Zhang, G. Tang, R. Li, Y. Chen, L. Li, J. Hu, J. Hong, Q. Chen, X. Gao, H. Zhou, Nat. Commun. 9 (2018) 2793.
[84] D.J. Kubicki, D. Prochowicz, A. Hofstetter, S.M. Zakeeruddin, M. Grätzel, L. Emsley, J. Am. Chem. Soc. 139 (2017) 14173-14180.
[85] M. Abdi-Jalebi, M.I. Dar, A. Sadhanala, S.P. Senanayak, M. Franckevičius, N. Arora, Y. Hu, M.K. Nazeeruddin, S.M. Zakeeruddin, M. Grätzel, R.H. Friend, Adv. Energy Mater. 6 (2016) 1502472.
[86] S.T. Williams, A. Rajagopal, S.B. Jo, C.C. Chueh, T.F.L. Tang, A. Kraeger, A.K.Y. Jen, J. Mater. Chem. A 5 (2017) 10640-10650.
[87] J. Liang, Z. Liu, L. Qiu, Z. Hawash, L. Meng, Z. Wu, Y. Jiang, L.K. Ono, Y.B. Qi, Adv. Energy Mater. 8 (2018) 1800504.
[88] M. Jahandar, J.H. Heo, C.E. Song, K.-J. Kong, W.S. Shin, J.-C. Lee, S.H. Im, S.-J. Moon, Nano Energy 27 (2016) 330-339.
[89] Z.-K. Wang, M. Li, Y.-G. Yang, Y. Hu, H. Ma, X.-Y. Gao, L.-S. Liao, Adv. Mater. 28 (2016) 6695-6703.
[90] J.T.-W. Wang, Z. Wang, S.K. Pathak, W. Zhang, D. deQuilettes, F. Wisnivesky, J. Huang, P. Nayak, J. Patel, h. yusof, Y. Vaynzof, R. Zhu, I. Ramirez, J. Zhang, C. Ducati, C. Grovenor, M. Johnston, D.S. Ginger, R. Nicholas, H. Snaith, Energy Environ. Sci. 9 (2016) 2892-2901.
[91] J.M. Ball, A. Petrozza, Nat. Energy 1 (2016) 16149.

[92] T.M. Brenner, D.A. Egger, L. Kronik, G. Hodes, D. Cahen, Nat. Rev. Mater. 1 (2016) 15007.
[93] J. Huang, Y. Yuan, Y. Shao, Y. Yan, Nat. Rev. Mater. 2 (2017) 17042.
[94] C. Ran, J. Xu, W. Gao, C. Huang, S. Dou, Chem. Soc. Rev. 47 (2018) 4581-4610.
[95] J.S. Park, S. Kim, Z. Xie, A. Walsh, Nat. Rev. Mater. 3 (2018) 194-210.
[96] L.K. Ono, S. Liu, Y.B. Qi, Angew. Chem. Int. Ed. (2019), DOI: 10.1002/anie.201905521.
[97] P.-K. Kung, M.-H. Li, P.-Y. Lin, Y.-H. Chiang, C.-R. Chan, T.-F. Guo, P. Chen, Adv. Mater. Interfaces (2018) 1800882.
[98] P. Zhao, B.J. Kim, H.S. Jung, Mater. Today Energy 7 (2018) 267-286.
[99] D. Meggiolaro, E. Mosconi, F. De Angelis, ACS Energy Lett. 4 (2019) 779-785.
[100] K. Zhu, S. Cong, Z. Lu, Y. Lou, L. He, J. Li, J. Ding, N. Yuang, M.H. Rümmeli, G. Zou, J. Power Sources 428 (2019) 82-87.
[101] Z. Wu, S.R. Raga, E.J. Juarez-Perez, X. Yao, Y. Jiang, L.K. Ono, Z. Ning, H. Tian, Y.B. Qi, Adv. Mater. (2017) 1703670.
[102] C.-T. Lin, F. De Rossi, J. Kim, J. Baker, J. Ngiam, B. Xu, S. Pont, N. Aristidou, S.A. Haque, T. Watson, M.A. McLachlan, J.R. Durrant, J. Mater. Chem. A 7 (2019) 3006-3011.
[103] X. Zheng, Y. Deng, B. Chen, H. Wei, X. Xiao, Y. Fang, Y. Lin, Z. Yu, Y. Liu, Q. Wang, J. Huang, Adv. Mater. 30 (2018) 1803428.
[104] F. Zhang, D. Bi, N. Pellet, C. Xiao, Z. Li, J.J. Berry, S.M. Zakeeruddin, K. Zhu, M. Grätzel, Energy Environ. Sci. 11 (2018) 3480-3490.
[105] E.J. Juarez-Perez, L.K. Ono, M. Maeda, Y. Jiang, Z. Hawash, Y.B. Qi, J. Mater. Chem. A 6 (2018) 9604-9612.
[106] L. Wang, H. Zhou, J. Hu, B. Huang, M. Sun, B. Dong, G. Zheng, Y. Huang, Y. Chen, L. Li, Z. Xu, N. Li, Z. Liu, Q. Chen, L.-D. Sun, C.-H. Yan, Science 363 (2019) 265-270.
[107] S. Wang, Y. Jiang, E.J. Juarez-Perez, L.K. Ono, Y.B. Qi, Nat. Energy 2 (2016) 16195.
[108] Z. Liu, J. Hu, H. Jiao, L. Li, G. Zheng, Y. Chen, Y. Huang, Q. Zhang, C. Shen, Q. Chen, H. Zhou, Adv. Mater. 29 (2017) 1606774.
[109] J. Xu, A. Buin, A.H. Ip, W. Li, O. Voznyy, R. Comin, M. Yuan, S. Jeon, Z. Ning, J.J. McDowell, P. Kanjanaboos, J.-P. Sun, X. Lan, L.N. Quan, D.H. Kim, I.G. Hill, P. Maksymovych, E.H. Sargent, Nat. Commun. 6 (2015) 7081.
[110] X. Zheng, B. Chen, J. Dai, Y. Fang, Y. Bai, Y. Lin, H. Wei, Xiao C. Zeng, J. Huang, Nat. Energy 2 (2017) 17102.
[111] Q. Wang, B. Chen, Y. Liu, Y. Deng, Y. Bai, Q. Dong, J. Huang, Energy Environ. Sci. 10 (2016) 516-522.

[112] Z. Chen, B. Turedi, A.Y. Alsalloum, C. Yang, X. Zheng, I. Gereige, A. AlSaggaf, O.F. Mohammed, O.M. Bakr, ACS Energy Lett. 4 (2019) 1258-1259.
[113] Y. Liu, Z. Yang, S. Liu, Adv. Sci. 5 (2018) 1700471.
[114] Y. Liu, Q. Dong, Y. Fang, Y. Lin, Y. Deng, J. Huang, Adv. Funct. Mater. (2019) 1807707.
[115] S. Li, C. Zhang, J.-J. Song, X. Xie, J.-Q. Meng, S. Xu, Crystals 8 (2018) 220.
[116] X.-D. Wang, W.-G. Li, J.-F. Liao, D.-B. Kuang, Solar RRL 3 (2019) 1800294.
[117] L.K. Ono, T. Kim, Y. Jiang, Y.B. Qi, S.F. Liu, ACS Energy Lett. 3 (2018) 1898-1903.
[118] B. Lee, T. Hwang, S. Lee, B. Shin, B. Park, Sci. Rep. 9 (2019) 4803.
[119] S.R. Raga, M.-C. Jung, M.V. Lee, M.R. Leyden, Y. Kato, Y.B. Qi, Chem. Mater. 27 (2015) 1597-1603.
[120] Z. Xiao, Y. Yan, Adv. Energy Mater. 7 (2017) 1701136.
[121] H. Tan, A. Jain, O. Voznyy, X. Lan, F.P. García de Arquer, J.Z. Fan, R. Quintero-Bermudez, M. Yuan, B. Zhang, Y. Zhao, F. Fan, P. Li, L.N. Quan, Y. Zhao, Z.-H. Lu, Z. Yang, S. Hoogland, E.H. Sargent, Science 355 (2017) 722-726.
[122] T. Wu, Y. Wang, X. Li, Y. Wu, X. Meng, D. Cui, X. Yang, L. Han, Adv. Energy Mater. 9 (2019) 1803766.
[123] X. Gong, L. Guan, H. Pan, Q. Sun, X. Zhao, H. Li, H. Pan, Y. Shen, Y. Shao, L. Sun, Z. Cui, L. Ding, M. Wang, Adv. Funct. Mater. 28 (2018) 1804286.
[124] W.S. Yang, B.-W. Park, E.H. Jung, N.J. Jeon, Y.C. Kim, D.U. Lee, S.S. Shin, J. Seo, E.K. Kim, J.H. Noh, S.I. Seok, Science 356 (2017) 1376-1379.
[125] J.T.-W. Wang, Z. Wang, S. Pathak, W. Zhang, D.W. deQuilettes, F. Wisnivesky-Rocca-Rivarola, J. Huang, P.K. Nayak, J.B. Patel, H.A. Mohd Yusof, Y. Vaynzof, R. Zhu, I. Ramirez, J. Zhang, C. Ducati, C. Grovenor, M.B. Johnston, D.S. Ginger, R.J. Nicholas, H.J. Snaith, Energy Environ. Sci. 9 (2016) 2892-2901.
[126] F. Zheng, W. Chen, T. Bu, K.P. Ghiggino, F. Huang, Y. Cheng, P. Tapping, T.W. Kee, B. Jia, X. Wen, Adv. Energy Mater. 9 (2019) 1901016.
[127] L. Kuai, Y. Wang, Z. Zhang, Y. Yang, Y.B. Qin, T. Wu, Y. Li, Y. Li, T. Song, X. Gao, L. Wang, B. Sun, Solar RRL 3 (2019) 1900053.
[128] M. Abdi-Jalebi, Z. Andaji-Garmaroudi, A.J. Pearson, G. Divitini, S. Cacovich, B. Philippe, H. Rensmo, C. Ducati, R.H. Friend, S.D. Stranks, ACS Energy Lett. 3 (2018) 2671-2678.
[129] C. Liu, Z. Huang, X. Hu, X. Meng, L. Huang, J. Xiong, L. Tan, Y. Chen, ACS Appl. Mater. Interfaces 10 (2018) 1909-1916.

[130] D.W. de Quilettes, S.M. Vorpahl, S.D. Stranks, H. Nagaoka, G.E. Eperon, M.E. Ziffer, H.J. Snaith, D.S. Ginger, Science 348 (2015) 683-686.
[131] A.D. Jodlowski, C. Roldán-Carmona, G. Grancini, M. Salado, M. Ralaiarisoa, S. Ahmad, N. Koch, L. Camacho, G. de Miguel, M.K. Nazeeruddin, Nat. Energy 2 (2017) 972-979.
[132] B. Li, V. Ferguson, S.R.P. Silva, W. Zhang, Adv. Mater. Interfaces (2018) 1800326.
[133] R. Wang, M. Mujahid, Y. Duan, Z.-K. Wang, J. Xue, Y. Yang, Adv. Funct. Mater. (2019) 1808843.
[134] L. Meng, J. You, Y. Yang, Nat. Commun. 9 (2018) 5265.
[135] L. Qiu, L.K. Ono, Y.B. Qi, Mater. Today Energy 7 (2018) 169-189.
[136] L.K. Ono, Y.B. Qi, S. Liu, Joule 2 (2018) 1961-1990.
[137] N. Ahn, K. Kwak, M.S. Jang, H. Yoon, B.Y. Lee, J.-K. Lee, P.V. Pikhitsa, J. Byun, M. Choi, Nat. Commun. 7 (2016) 13422.
[138] N. Aristidou, C. Eames, I. Sanchez-Molina, X. Bu, J. Kosco, M.S. Islam, S.A. Haque, Nat. Commun. 8 (2017) 15218.
[139] G. Yang, P. Qin, G. Fang, G. Li, Solar RRL 2 (2018) 1800055.
[140] Y. Zong, Y. Zhou, Y. Zhang, Z. Li, L. Zhang, M.-G. Ju, M. Chen, S. Pang, X.C. Zeng, N.P. Padture, Chem 4 (2018) 1404-1415.
[141] W.-Q. Wu, Z. Yang, P.N. Rudd, Y. Shao, X. Dai, H. Wei, J. Zhao, Y. Fang, Q. Wang, Y. Liu, Y. Deng, X. Xiao, Y. Feng, J. Huang, Sci. Adv. 5 (2019) eaav8925.
[142] D.W. deQuilettes, S. Koch, S. Burke, R.K. Paranji, A.J. Shropshire, M.E. Ziffer, D.S. Ginger, ACS Energy Lett. 1 (2016) 438-444.
[143] H. Zhang, Y. Wu, C. Shen, E. Li, C. Yan, W. Zhang, H. Tian, L. Han, W.-H. Zhu, Adv. Energy Mater. 9 (2019) 1803573.
[144] D. Wei, F. Ma, R. Wang, S. Dou, P. Cui, H. Huang, J. Ji, E. Jia, X. Jia, S. Sajid, A.M. Elseman, L. Chu, Y. Li, B. Jiang, J. Qiao, Y. Yuan, M. Li, Adv. Mater. 30 (2018) 1707583.
[145] T.-H. Han, J.-W. Lee, C. Choi, S. Tan, C. Lee, Y. Zhao, Z. Dai, N. De Marco, S.-J. Lee, S.-H. Bae, Y. Yuan, H.M. Lee, Y. Huang, Y. Yang, Nat. Commun. 10 (2019) 520.
[146] X. Li, W. Zhang, Y.-C. Wang, W. Zhang, H.-Q. Wang, J. Fang, Nat. Commun. 9 (2018) 3806.
[147] M. Qin, J. Cao, T. Zhang, J. Mai, T.-K. Lau, S. Zhou, Y. Zhou, J. Wang, Y.-J. Hsu, N. Zhao, J. Xu, X. Zhan, X. Lu, Adv. Energy Mater. 8 (2018) 1703399.
[148] B. Dou, L.M. Wheeler, J.A. Christians, D.T. Moore, S.P. Harvey, J.J. Berry, F.S. Barnes, S.E. Shaheen, M.F.A.M. van Hest, ACS Energy Lett. 3 (2018) 979-985.

[149] W. Zhang, S. Pathak, N. Sakai, T. Stergiopoulos, P.K. Nayak, N.K. Noel, A.A. Haghighirad, V.M. Burlakov, D.W. deQuilettes, A. Sadhanala, W. Li, L. Wang, D.S. Ginger, R.H. Friend, H.J. Snaith, Nat. Commun. 6 (2015) 10030.

Graphical Abstracts

Additives in Metal Halide Perovskite Films and Their Applications in Solar Cells

Zonghao Liu[a,+], Luis K. Ono[a,+], Yabing Qi[a,*]

[a] *Energy Materials and Surface Sciences Unit (EMSSU), Okinawa Institute of Science and Technology Graduate University (OIST), 1919-1 Tancha, Onna-son, Kunigami-gun, Okinawa, 904-0495, Japan*

[*]Corresponding author: Yabing Qi, *E-mail address:* Yabing.Qi@OIST.jp

+These authors contributed equally to this work

This review summarizes recent progress on additive strategies employed for fabrication of large-scale perovskite solar cells and modules. Additives promote perovskite grain growth, defects reduction, and stability enhancement in addition to power-conversion-efficiency.